EXPLUME v1.0: a model for personal exposures to ambient O_3 and $PM_{2.5}$

Myrto Valari[1], Konstandinos Markakis[1], Emilie Powaga[2], Bernard Collignan[2], and Olivier Perrussel[3]

[1]LMD/IPSL, Laboratoire de Météorologie Dynamique, Sorbonne Université, Ecole Polytechnique, IPSL Research University, Ecole Normale Supérieure, CNRS, 75252 Paris, France

[2]Université Paris-Est, Centre scientifique et Technique du Bâtiment, Direction Santé Confort, Division Physico-chimie - Sources et Transferts de polluants

[3]AIRPARIF, Association de surveillance de qualité de l'air en Île-de-France, 7 rue Crillon, 75004, Paris, France

Correspondence: Myrto Valari (myrto.valari@lmd.polytechnique.fr)

Abstract. This paper presents the first version of the regional scale personal exposure model EXPLUME. The model uses simulated gridded data of outdoor O_3 and $PM_{2.5}$ concentrations and several population and building-related datasets to simulate 1) space-time activity event sequences, 2) the infiltration of atmospheric contaminants indoors and 3) daily aggregated personal exposures. The model is applied over the greater Paris region at 2km x 2km resolution for the entire 2017 year. Annual averaged population exposures are discussed. We show that population mobility within the region, disregarding pollutant concentrations indoors, has only a small effect on average daily exposures. By contrast, considering the infiltration of $PM_{2.5}$ in buildings decreases annual average exposure by 11% (population average). Moreover, accounting for $PM_{2.5}$ exposure during transportation (in-vehicle, while waiting on subway platforms, and while crossing on-road tunnels) increases average population exposure by 5%. We show that the spatial distribution of $PM_{2.5}$ and O_3 exposures is similar to the concentration maps over the region, but the exposure scale is very different when accounting for indoor exposure. We model large intra-population variability in $PM_{2.5}$ exposure as a function of the transportation mode, especially for the upper percentiles of the distribution. 20% of the population using bicycles or motorcycles is exposed to annual average $PM_{2.5}$ concentrations above the EU target value (25 $\mu g/m^3$), compared to 0% for people travelling by car. Finally, we develop a 2050-horizon projection of the building stock to study how changes in the buildings' characteristics to comply with the thermal regulations will affect personal exposures. We show that exposure to ozone will decrease by as much as 14% as a result of this projection, whereas there is no significant impact on exposure to $PM_{2.5}$.

1 Introduction

Air pollution is the first environmental health risk with significant effects on morbidity and mortality (Lim et al., 2012; WHO, 2014). Despite significant improvement in European air-quality over the past decades, in 2017 approximately 77% of the urban population was still exposed to $PM_{2.5}$ concentrations exceeding the WHO Air Quality Guidelines for health (14% for O_3) (EEA, 2019). More than half of the mortality burden attributed to exposure to suspended particles of an aerodynamic diameter less than 2.5 $\mu g/m^3$ ($PM_{2.5}$) in France, occurs in cities of more than 100 000 inhabitants (Pascal et al., 2016). Several

epidemiological studies have shown the adverse health effects of exposure to $PM_{2.5}$. For instance in France, in 2004–2006, about 3000 deaths per year were attributed to levels of PM2.5 exceeding the WHO guideline value in nine French urban areas participating in the Aphekom project (Pascal et al., 2013). Previous studies have shown that ozone exposures correlate with both morbidity and mortality (Sun et al., 2018; Di et al., 2017).

In the majority of these studies, the exposure surrogate associated with morbidity or mortality metrics is a spatially aggregated pollutant concentration from measurements at different sites over the urban agglomeration (Anderson et al., 2004; Bell et al., 2005). The underlying hypothesis here is that exposure is homogenous over the population. For this assumption to be valid, these studies are limited to small geographical zones where population density and pollutant concentrations are also homogenous (Sarnat et al., 2007). Several shortcomings of this approach have been raised in previous studies. On one hand, pollutant concentrations are spatially heterogeneous, especially within cities where different emission sources co-exist and the presence of buildings imposes barriers to the dispersion of pollutants. For example, a Health Effects Institute report states that the zones most impacted by traffic-related pollution are up to 300–500m from highways and other major roads, and when calculated for large cities in North America that affects 30 – 45% of the population (HEI, 2010). Intra-urban variability in pollutant concentration is a principal source of exposure misclassification in environmental epidemiology models, leading to errors in the evaluation of the health risk (Blair et al., 2007; Edwards and Keil, 2017). Furthermore, large variability in population exposure arises from human activity, population mobility, transport usage, building characteristics (Georgopoulos et al., 2005). Therefore, to study the health risk on specific population groups — such as children, elderly people, asthma patients or pregnant women (Olsson et al., 2014) or the health effect of co-pollutants (Olstrup et al., 2019b, a; Valari et al., 2011), or the risk associated to living or working near busy roads (Lipfert and Wyzga, 2008; Miranda et al., 2013) — one has to account for pollutant concentration at district-level, population dynamics, and exposure indoors and during transport (Franklin et al., 2012; Hodas et al., 2012).

To answer this emerging demand, several methods for estimating personal exposure have been developed. Land-use regression models have been largely used to relate concentrations measured at monitor sites with concentration estimates at different locations across the city (Beelen et al., 2013; Cattani et al., 2017; Ryan and LeMasters, 2007). Then, space-time activity data are coupled to concentration data to provide exposure estimates (Vizcaino and Lavalle, 2018; Xu et al., 2019a). Land-use regression models provide spatial maps where urban features such as roads, buildings, parks may be distinguished from background concentration levels. But concentration gradients resulting from the regression do not account for the dynamical or chemical processes taking place at these scales. Portable instruments, based on mass filters or high-accuracy optical methods (reference sensors) have also been used during specific field campaigns to to measure exposure in cars, in subway trains and on subway platforms, and in residences or other indoor micro-environmental locations (Hwang and Lee, 2018; Lim et al., 2012; Morales Betancourt et al., 2019; Williams and Knibbs, 2016; Xu et al., 2019b). These methods are accurate but restricted to limited periods and spatial contexts. The availability of low-cost personal monitors (micro-sensors) is a new opportunity in the atmospheric exposure field. They provide access to almost real-time, high resolution concentration measurements (Xie et al., 2017). However, the accuracy of these instruments, their calibration, as well as their high sensitivity to environmental

conditions (e.g. humidity) and human manipulation are yet to be addressed before their true potential to be realized (Berchet et al., 2017).

Pollutant concentration fields simulated with atmospheric dispersion models are another possible input source for exposure models. The advantage of this approach is that simulation data may cover long time-periods to support climate studies or policy applications adjusting for meteorological variability, emissions regulations, and land-use classification. Gaussian dispersion models have often been coupled with population space-time activity data for use in exposure studies (Dias and Tchepel, 2018; Korek et al., 2015; Batterman et al., 2014; Willers et al., 2013). These models, coupled with regional-scale chemistry-transport models, account simultaneously for long-range transport, regional background concentrations, and local features such as traffic emissions over the road network (Soares et al., 2014).

Regional scale chemistry-transport models (CTMs) such as CHIMERE (Mailler et al., 2017) or CMAQ (K. Wyat Appel et al., 2014) have achieved resolution of 1km x 1km with sufficient accuracy to be considered for use in such fine scale applications (Beevers et al., 2013). Statistical, dynamical or hybrid downscaling techniques such as kriging (Beauchamp et al., 2015) or subgrid-scale parametrizations (Valari and Menut, 2010) can be applied or coupled to these models to provide concentrations at district level. The use of CTMs instead of high-resolution Gaussian or Lagrangian models in an exposure context has several advantages. The study domain may be large enough to cover an entire region, whereas typical Gaussian or Lagrangian applications cover at best, the urban agglomeration. However, a large part of the population moves in and out of the agglomeration within the day and on systematic basis. Furthermore, the enhanced chemical mechanisms of CTMs compared to the simplified chemistry (the Chapman cycle) in Gaussian or Lagrangian models gives access to refined information on the chemical speciation and size distribution of particulate matter (PM). This information is particularly relevant in the context of health impact assessment, since the health impact of PM strongly depends on these properties (Atkinson et al., 2015; Cassee et al., 2013).

This paper presents the first version of a regional scale model for personal exposures to O_3 and $PM_{2.5}$. The originality of the model lies on the development of i) individual activity sequences that are defined geographically in space and time and ii) the modelling of seasonal distributions of indoor/outdoor ratios by building type and age. This latter feature is unique in personal exposure modelling since typically, indoor pollutant concentrations relie on measurements for a few locations that may not represent the area's buildings. The model is developed as a post-processing tool for the CHIMERE regional scale CTM and aims to facilitate health impact assessment. Outdoor pollutant concentrations are simulated with CHIMERE at 2km x 2km resolution. The model selects sample populations that reproduce essential demographics at relevant geographical units (communes), namely age, gender, occupation, communes of residence and work, principal modes of transportation and construction dates of residence and workplace. Activity event sequences for each member of the sample are developed by matching the distributions in the simulated population with distributions in the Enquête Globale de Transport (EGT, 2010) study. Infiltration of outdoor air-pollution indoors in dwellings, offices, and schools, is modeled with the SIREN model (Collignan et al., 2012), developed at the Centre Scientifique et Technique du Bâtiment (CSTB). SIREN is used to develop seasonal distributions of indoor/outdoor ratios for each type of building. For other indoor locations (cars, buses, subway and regional trains and tram) we apply indoor/outdoor ratios found in the literature from previous measurement campaigns conducted in the region. Ad-

justments are also applied for specific activities such as cycling, walking on busy roads, waiting at the subway platforms, as well as for car journeys that intersect tunnels or the Boulevard Periphèrique (ring road). Space-time activity sequences define the geographical coordinates of each member of the population at each minute of the simulation. Daily averaged personal exposures are calculated from the products of time spent by a person in different microenvironments and the time-averaged pollutant concentrations occurring in those locations (Klepeis, 2006). Personal exposures are simulated for the entire 2017 year over the Ile-de-France region (greater Paris).

2 Personal exposure calculation

The most accurate exposure assessment would rely on real-time personal monitoring devices affixed to people as they move within all the locations that are part of their daily routines (Klepeis, 2006). In practice, such equipment is too expensive to affix to large cohorts. Also questions such as the calibration of the monitors and the assessment of the uncertainties still need to be tackled before such studies could be carried out at regional scale. In a modeling framework, discrete locations termed as microenvironments are considered rather than fully continuous space. In this case, the exposure trajectory of the receptor is followed explicitly. This approach has been adapted in cohort studies such as McBride et al. (2007). As in Klepeis (2006), in the exposure model developed here receptors are simulated through individuals. Further discretizing in time, we calculate exposure as the sum of the product of time spent by a person in different microenvironments and the time-averaged pollutant concentrations occurring in those locations:

$$E_i = \sum_{j=1}^{m} C_{ij} T_{ij} \tag{1}$$

Here T_{ij} is the time spent in microenvironment j by person i with units in minutes, C_{ij} is the air-pollutant concentration person i experiences in microenvironment j in units of [μg/m^3], E_i is the integrated exposure for person i [μg/m^3 min], and m the number of different microenvironments. In this formulation, concentration C_{ij} is averaged over the corresponding time period T_{ij} .

The general structure of the model with the necessary input datasets for the exposure calculation is illustrated in Figure 1. Outdoor pollutant concentrations are simulated with a regional scale chemistry-transport model. We use hourly averaged data over a horizontal grid with 2km spacing in both the west-east and the south-north directions (Section 3.1). Indoors pollutant concentrations(in buildings and during transportation) are deduced from outdoor concentrations by applying indoor/outdoor ratios. The model does not account for indoor sources so far. For buildings, indoor/outdoor ratios are calculated through a ventilation model (Section 3.2.1). For other indoor microenvironments, indoor/outdoor ratios are either taken from previous studies in the Ile-de-France region or calculated from existing indoor and outdoor concentration data as is the case for subway platforms (Section 3.2.2).

To obtain activity event sequences that determine the location of each member of the simulated population in time we draw on the 2010 survey “Enquête globale de transport” (EGT, 2010) conducted by the Direction Régional et Interdépartemental de l'Equipement et de l'Aménagement d'Ile-de-France. This survey questioned 43 000 individuals and identified 143 000 journeys.

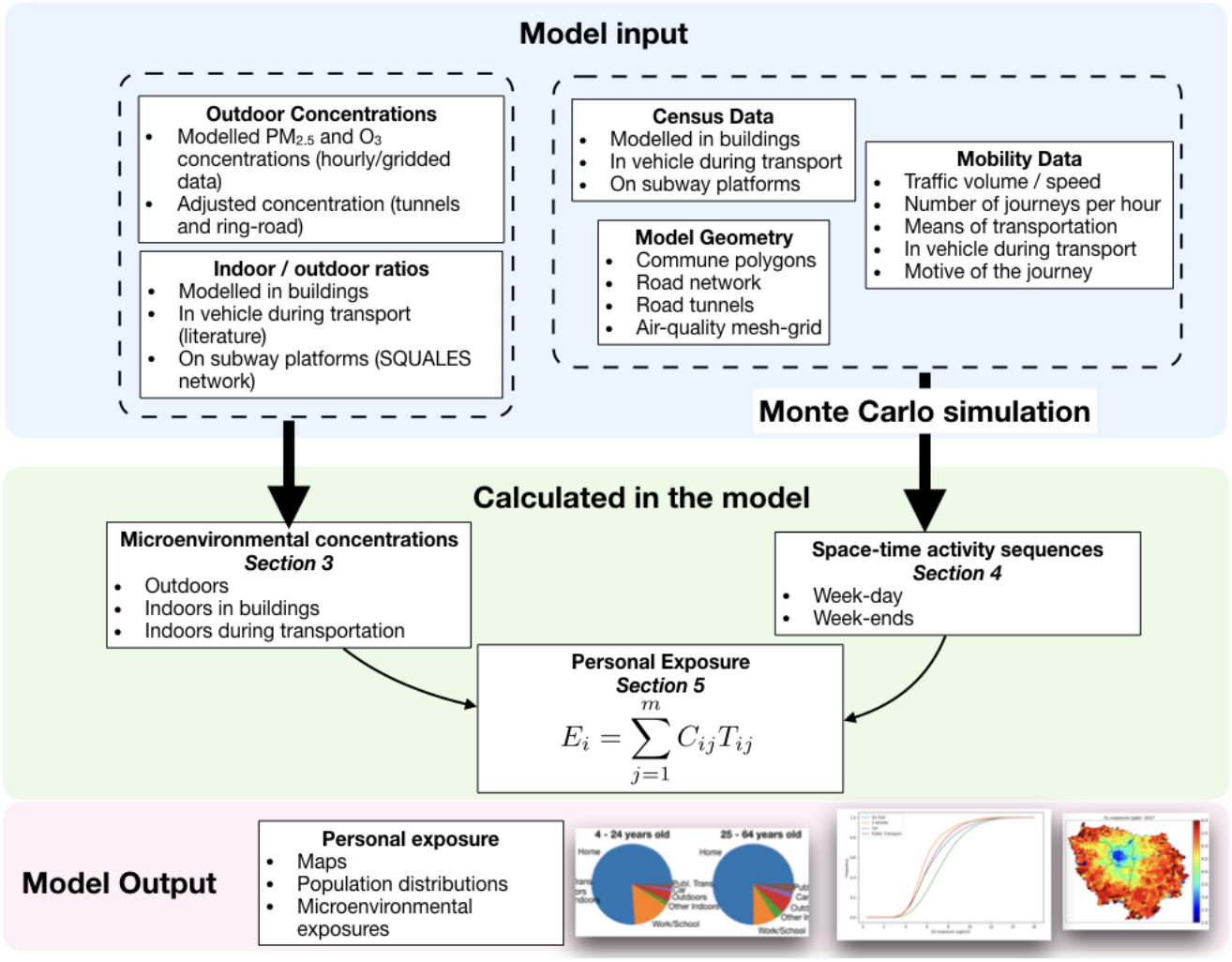

Figure 1. *Overview of the EXPLUME model structure, from the input data to the exposure calculation.*

Each journey is characterized by the origin and destination points, the motive for traveling, the duration and the means of transportation used. The mobility of the sample population is simulated with a Monte Carlo model that matches the simulated data with the EGT (2010) data (Section 4).

3 Pollutant concentrations

3.1 Outdoor O_3 and $PM_{2.5}$ concentration predictions

Pollutant concentrations are modeled with the CHIMERE model (Mailler et al., 2017) at a horizontal resolution of 2km x 2km. Four-level one-way nesting is used for the CHIMERE simulation with grids of 60, 20, 7 and 2km spacing between cells at both west-east and south-north directions. 15 vertical layers are used from 998 up to 300hPa with layers becoming thicker with distance from the surface level. Meteorological conditions are modeled with the Weather Research and Forecasting model (Skamarock et al., 2008) off-line at the same 4-level nesting grids as for the CHIMERE simulation but with a two-way nesting configuration. Global HTAP (Hemispheric Transport of Atmospheric Pollutants) anthropogenic emissions are used outside the European continent, EMEP emissions for Europe outside the Ile-de-France region and finally a 1km x 1km resolution bottom up emission inventory developed by the AIRPARIF agency for anthropogenic emissions over the Ile-de-France region.

Table 1. Common metrics of statistical performance of the CHIMERE model, namely Pearson correlation, mean bias and root mean square error, aggregated over the whole 2017 year and for summer and winter seasons. Comparisons with traffic background and rural stations are conducted separately.

	O_3 hourly [ppb]		**$PM_{2.5}$ hourly [μg/m^3]**	
	Urban background (15 sites)	**Rural (7 sites)**	**Urban background (6 sites)**	**Traffic (4 sites)**
YEAR / Pears. Cor. [non dim.]	0.74	0.74	0.55	0.57
YEAR / Mean Bias	0.06	0.95	2.14	-1.91
YEAR / RMSE	10.25	9.6	11.8	12.7
SUMMER / Pears. Cor. [non dim.]	0.72	0.75	0.19	0.23
SUMMER / Mean Bias	0.79	2.58	0.19	-3.48
SUMMER / RMSE	10.7	10.1	5.4	7.3
WINTER / Pears. Cor. [non dim.]	0.58	0.62	0.56	0.59
WINTER / Mean Bias	-0.73	1.9	0.74	-1.35
WINTER / RMSE	9.7	9.7	16.8	18.1

Table 1 summarizes the comparison between the 2017-year simulation against measurements at all the available monitor sites of the AIRPARIF air-quality network. Urban monitoring-sites are divided into two groups : traffic sites are located on the road network and have a relatively small spatial representativeness, whereas urban background stations are located away from the road network and their spatial representativeness spans over larger areas. Rural monitor sites are located outside the city and have the largest spatial representativeness. A good temporal correlation on an hourly basis is observed for ozone, especially for summer periods on both urban background and rural locations. The correlation is lower for the winter period. Afternoon ozone concentrations are underestimated over urban background stations as also shown in Figure 2. This is due to model's

horizontal resolution that is too coarse to spatially resolve the fast NO-titration near high emission sources. On the contrary, day-time ozone is slightly overestimated over rural locations see Figure S1 (supplemental material). In both urban background and rural locations, night-time ozone is largely overestimated. The model keeps bringing ozone at the surface layer from the stratosphere and ozone accumulates in the surface layer in the absence of local NO emissions and dry deposition that remove it during day-time.

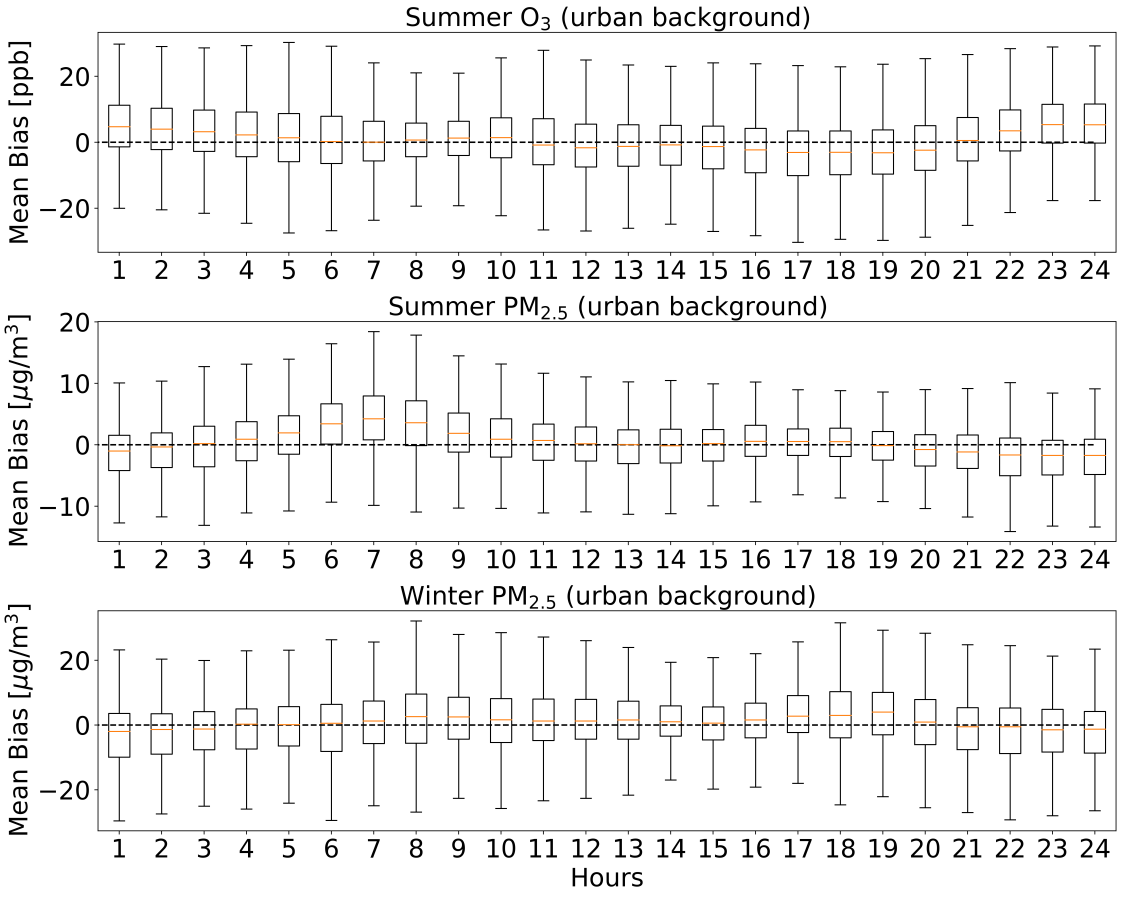

Figure 2. *Hourly mean bias of simulated surface O_3 (summer) and $PM_{2.5}$ (summer and winter) concentrations calculated during the year 2017 over 15 and 6 urban background monitor sites respectively.*

Temporal correlation, on an hourly basis, between simulated and observed $PM_{2.5}$ concentrations is much better for winter than for summer. Pearson correlation over urban background sites drops from 0.56 for the winter period to 0.19 for summer. The CHIMERE model overestimates $PM_{2.5}$ concentrations over urban sites and underestimates them over traffic stations (table 1 and Figure S2). Road transport is a major source of fine particles in urban areas. The 2km x 2km horizontal resolution is insufficient to reproduce the high $PM_{2.5}$ concentrations near these sources. Another possible reason for model's underestima-

tion of $PM_{2.5}$ concentrations over traffic stations is a poor representation of secondary organic aerosol formation near traffic emissions. The distribution of the above statistics across sites is shown in Figure S2 (supplemental material). As shown there, the underestimation of $PM_{2.5}$ concentrations over traffic sites may be particularly high.

Globally, we assume that the CHIMERE model at 2km x 2km resolution provides reliable O_3 and $PM_{2.5}$ background concentrations, being able to spatially differentiate the urban agglomeration from peri-urban and remote rural locations for $PM_{2.5}$ (Figure 3). The formation of well-structured ozone plumes over the rural area is also well represented as shown in the top left panel, where specific date/hour surface ozone concentration map is shown. The model is also capable of reproducing the diurnal cycle of ozone and $PM_{2.5}$. Pollutant episodes induced by favorable meteorological conditions are also well-captured by the model, even though a trend to underestimate ozone peaks and overestimate $PM_{2.5}$ peaks is observed.

Based on this analysis, for the personal exposure calculation we use simulated background O_3 and $PM_{2.5}$ concentrations from the CHIMERE model grid-cell where the activity takes place. Over the road network, where we know that the 2kmx2km CHIMERE model resolution is insufficient to reproduce the high $PM_{2.5}$ concentration levels, we apply correction coefficients to increase modeled concentrations. This happens in two cases: the Boulevard Periphérique (road ring) and inside road tunnels (see Section 3.2.2). Therefore, no stochastic selection operates for the estimation of outdoor pollutant concentrations.

3.2 Infiltration of outdoor O_3 and $PM_{2.5}$ indoors

3.2.1 Dwellings, offices and schools

Indoor pollutant concentration levels depend on indoor sources and on outdoor pollutants entering the building through natural or mechanical ventilation. As air flows through the envelope of the building, pollutants react with the surfaces over which they flow. Therefore, the actual flow indoors depends on the specific path that the air flow takes: permeability of the building shell, natural air entry, or ducts (Walker and Sherman, 2013). Other sinks of pollutants indoor are deposition on the indoor surfaces and chemical reactions with other indoor species. The relationship between these sources and sinks is expressed through equation 2 as in Walker et al. (2009).

$$\frac{dC_{X,in}}{dt} = \sum_i (P_{X,i} Q_{in,i}) \cdot C_{X,out} - (Q_{out} + \eta Q_h) C_{X,in} - k_d C_{X,in} - \sum_j k_j [chem_j] + \frac{C_X}{V} \quad (2)$$

Here,

- $C_{X,in}$ and $C_{X,out}$ are the concentrations of pollutant X indoors and outdoors respectively ($\mu g/m^3$)
- $P_{X,I}$ is the dimensionless penetration factor for the pollutant X through leak path i, i.e the fraction of the pollutant in the infiltration air that passes through the building shell or air entrance
- $Q_{in,i}$, Q_{out}, Q_h are, respectively the volume-normalized air flow rates into the building through path i, out of the building, and through the heating ventilating and air-conditioning equipment expressed in Air Changes per Hour units (h^{-1})
- η is the removal efficiency on the heating ventilating and air-conditioning equipment

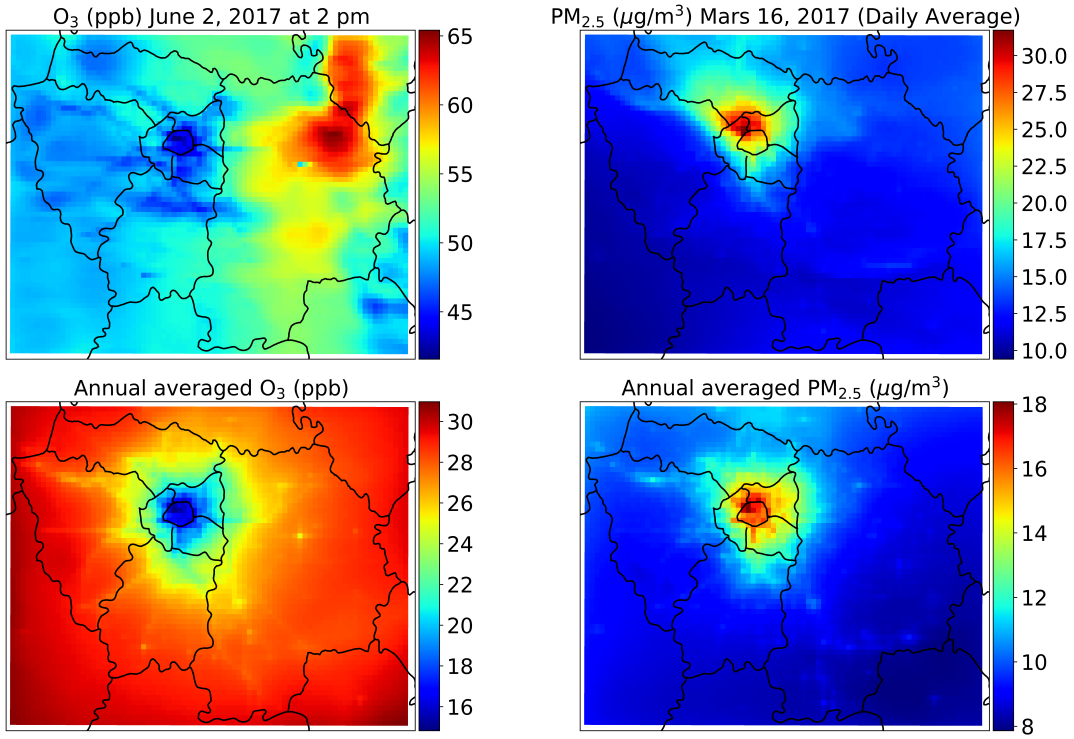

Figure 3. *Surface O_3 (left) and $PM_{2.5}$ (right) concentrations modeled with the CHIMERE chemistry-transport model. Maps on top show example of hourly averaged O3 concentration (left) and daily averaged $PM_{2.5}$ concentration (right) for specific hour/date. Maps on the bottom are annual averaged concentrations.*

- k_d is the indoor deposition loss rate coefficient (h^{-1})
- $chem_j$ is the concentration of the j^{th} chemical species reacting with the X pollutant (μg/m3)
- k_j the second order rate constant for the j reaction (h^{-1})
- S_X is the time varying indoor production rate (μg/h)
- V the volume (m^3)

Several studies have measured indoor/outdoor ratios for different building types and meteorological conditions, in cities around the world for ozone (Collignan et al., 2012; J., 2000) and airborne particles (Cyrys et al., 2004; Matson, 2005; Monn, 2001). Results show a strong dependence on the building usage (residence or office/school), the air-tightness of the building, the ventilation system ,and the proximity to atmospheric pollution sources. Ozone I/O ratios generally vary between 0.2 and 0.7 (J., 2000), while for $PM_{2.5}$, in the absence of indoor sources, between 0.5 and 1 (L. Morawska, C. He, 2003).

To account for the variability in I/O ratios due to these factors, we modelled ozone and fine airborne particles ($PM_{2.5}$) I/O ratios with the building ventilation model developed at the Centre Scientifique et Technique du bâtiment (CSTB), called SIREN (Collignan et al., 2012). The differential equation 2 is reformulated based on three assumptions: i) no indoor sources for O_3 and $PM_{2.5}$; ii) no chemical reactions with other atmospheric contaminants indoors; and iii) initial concentration indoors is null. We conducted simulations for a typical dwelling and office/school.

To account for the variability of I/O ratios due to air-tightness and ventilation systems, we applied a classification of the building stock based on the construction date. This information integrates air-tightness and ventilation systems evolution based on the national thermal and ventilation regulations (ADEME, 2013), the evolution of the building stock as described in (INSEE, 2014), and the use of ventilation systems in French buildings (OQAI, 2006). Table 2 shows the applied parametrizations for the different usages and construction dates. The values of air-tightness range from 2.5 $m^3/h/m^2$, representative of old leaky buildings to 0.6 $m^3/h/m^2$ corresponding to air-tight new constructions. A sensitivity analysis with the SIREN model showed that I/O ratio for O_3 decrease from 0.3 for the leaky building to 0.2 for the air-tight building and from 1 (air-tight building) to 0.8 (leaky building) for $PM_{2.5}$. Based on the INSEE (2014) data, the percentages of dwellings constructed before 1974 in the non-thermally rehabilitated and thermally rehabilitated classes are 25% and 75% respectively. No thermal rehabilitation is applied on offices and schools constructed before 1974. The air-tightness and ventilation systems for offices and schools built after 2012 do not change but the proportion of buildings in this category increases with time.

Climatological conditions, temperature, pressure, and outdoor pollutant concentrations are simulated with atmospheric models (WRF for meteorology and CHIMERE for ozone and $PM_{2.5}$ concentrations) at a 4x4km^2 horizontal resolution for a ten-year period from 1991 to 2000. Atmospheric fields are spatially averaged over the eight departments of the region. So, the atmospheric conditions database input for the SIREN model consists of ten-year period hourly data for the eight departments of the Ile-de-France region.

For each Ile-de-France department eight SIREN simulations are conducted (five for dwellings and three for office/schools) at a 3 min time-step. Penetration factor is fixed to 0.8 through the building shell and 1 through air inlet based on the state of the art (Chen and Zhao, 2011; Monn, 2001; Stephens et al., 2012; Thatcher et al., 2003). Confronting numerical simulations with SIREN and I/O ratio measurements the deposition rate was fixed to 0.1 h^{-1}. The SIREN model output consists of a decade long database of I/O ratios for ozone and $PM_{2.5}$ at 3 min resolution for each of the eight Ile-de-France departments, for five construction date classes for dwellings and 3 construction date classes for offices and schools. This database is further processed to provide seasonal I/O ratios for each pollutant, building type, construction date, and geographical zone as shown in Figure 4. Indoor/outdoor ratios for the personal exposure calculation are drawn randomly from the corresponding seasonal distribution depending on the personal profile and month.

3.2.2 Transportation

Ambient concentrations inside the principal transportation modes are deduced from outdoor concentrations by adjusting for indoor/outdoor coefficients taken from a study dedicated to evaluating the pollutant levels to which the Ile-de-France citizens are exposed while commuting to work and back during morning and evening rash hours (Delaunay C. et al., 2012). A significant

Table 2. Parametrization of the SIREN ventilation model depending on the construction date and the type of building, referring to the buildings' air-tightness and the ventilation system.

	Dwelling		**Office/Scool**	
	Air-tightness under 4 Pa depressurization	Ventilation	Air-tightness under 4 Pa depressurization	Ventilation
Before 1974 not thermally rehabilitated	2.5 $m^3/h/m^2$	Natural ventilation based on the principle of rooms ventilated separately	2.5 $m^3/h/m^2$	No ventilation system
Before 1974 thermally rehabilitated	1.7 $m^3/h/m^2$	Natural ventilation based on the principle of rooms ventilated separately	NA	NA
1974 - 2005	1.7 $m^3/h/m^2$	Cross ventilation principle induced by an exhaust mechanical ventilation system	2.0 $m^3/h/m^2$	Cross ventilation principle by separated room induced by an exhaust mechanical ventilation system
2006 - 2012	1.0 $m^3/h/m^2$	Cross ventilation principle induced by an exhaust mechanical ventilation system	1.5$m^3/h/m^2$	Cross ventilation principle induced by a double flow mechanical ventilation system
After 2012	0.6 $m^3/h/m^2$	Cross ventilation principle induced by a double flow mechanical ventilation system	NA	NA

number of contrasting situations is retained; twenty routes are chosen implementing the main modes of transport: car, bus, subway, tramway, cycling and walking. Each route has been reproduced 30 times (15 round trips). The measurement campaign took place during the winter period of 2007 and 2008.

To define the indoor/outdoor ratio for each journey in the model we chose a random number within a uniform distribution between the minimum and maximum values obtained by the study of Delaunay C. et al. (2012). The extreme values of these distributions are shown in Table 3. For public transport we distinguish between waiting on the platform and journey. For the suburban train (RER), we distinguish between journeys inside the subway network in the Paris agglomeration and the rest of the

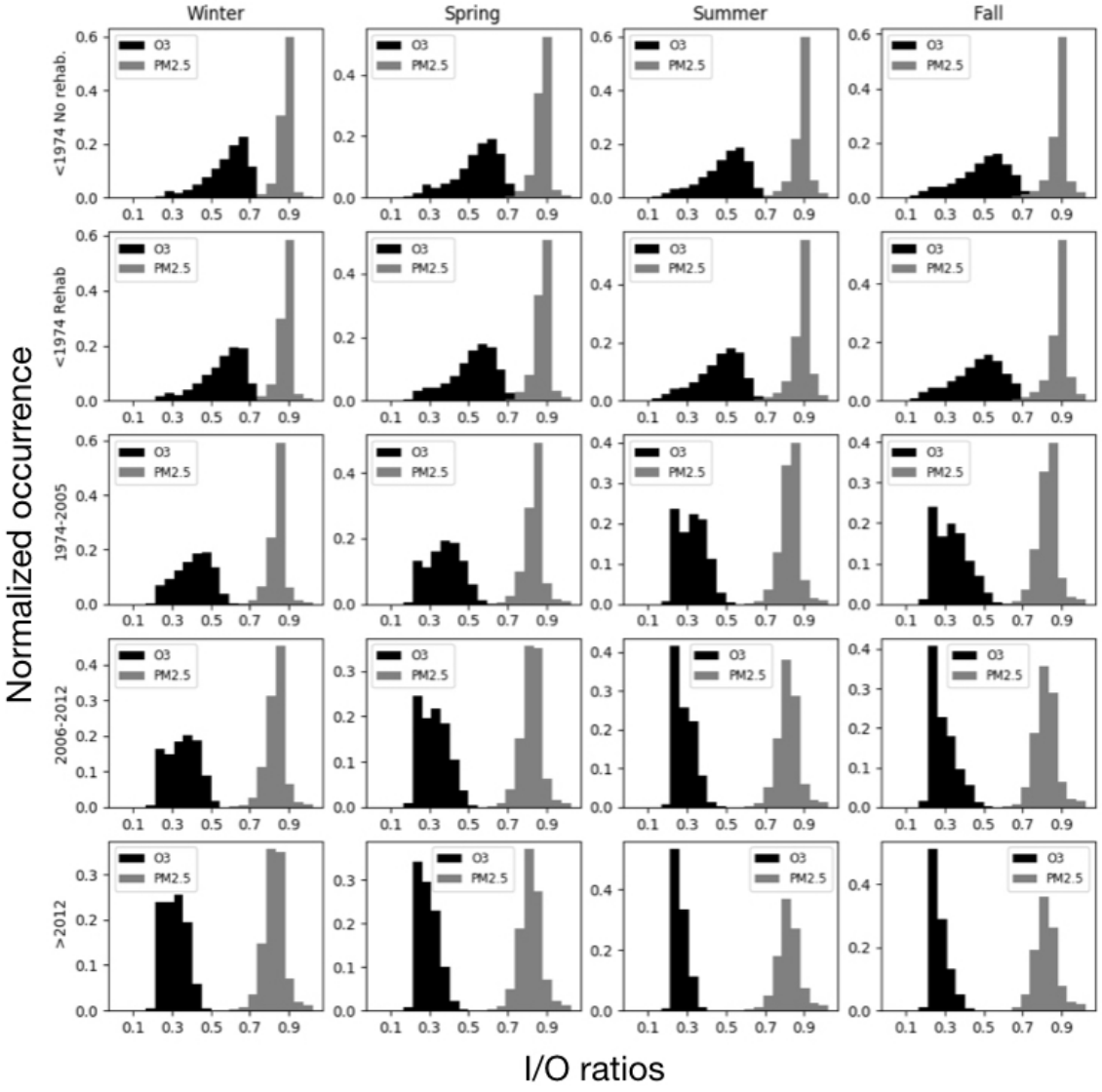

Figure 4. *O_3 and $PM_{2.5}$ indoor/outdoor ratios modeled with the SIREN model for dwellings (unitless). The number of occurrences of the histogram is normalized over the size of the dataset.*

235 network. For journeys in cars, we distinguish between the road network in the Paris agglomeration, the Boulevard Periphèrique (road ring), and the rest of the network (rural).

Several studies have shown that pollutant concentrations measured inside tunnels are several times higher than concentrations over the road but outside the tunnel. Orru H, B. Lövenheim, C. Johansson, B. Forsberg (2015) conducted a study to evaluate the health impact of the exposure to traffic exhaust inside road tunnels. Here, we apply a special adjustment for car journeys

Table 3. O_3 and $PM_{2.5}$ indoor / outdoor ratios for the principal means of transportation.

	Waiting		**Journey**	
	O_3	**$PM_{2.5}$**	**O_3**	**$PM_{2.5}$**
Subway	1	1	0	1.7-3.7
Bus	0	SQUALES	0	5.5-8.5
Tram	0	SQUALES	0	5.5-8.5
On foot	0	SQUALES	0	5.5-8.5
Two wheels	0	SQUALES	0	5.5-8.5
	Paris intra-muros/outside			
RER	0/1	SQUALES/1	0/0	3.2-5.4 / 2.9-3.2
	O_3	**$PM_{2.5}$**		
		Rural	**Boulevard Periphérique**	**Paris agglomeration**
Car	0	0.9-2	0.9-2.1	0.9-3.3

that cross tunnels. We assume that if the itinerary of an individual intersects a grid cell (2km x 2km) containing a tunnel, there is a 20% probability that the driver will pass through the tunnel. Due to lack of actual data this number is assigned here in an arbitrary manner. Further investigation in traffic data could provide a more accurate estimate of this probability. Based on the measurement campaign described in AIRPARIF (2009), we assume that the $PM_{2.5}$ concentration inside road-tunnels is two times higher than the outdoors concentration (see also Section 2).

$PM_{2.5}$ concentrations in the subway train tunnels are particularly high, especially for lines with rubber-tyred railway vehicles. To keep a record of the air-quality in the subway platforms the RATP (Régie Autonome des Transports Parisiens) operates measurements on a 24-hour basis at two metro stations and one RER platform (SQUALES). We used hourly on-platform measurements of the SQUALES network and outdoor concentration measurements from the AIRPARIF network for the entire 2013 year to establish a diurnal cycle of the indoor /outdoor ratio inside the subway platforms (Figure 5). For the personal exposure calculation, we draw a random value from the hourly distributions of indoor/outdoor ratios.

3.2.3 Other indoors

The SIREN model provides indoor /outdoor ratios for dwellings, offices and schools (Section 3.2.1). For other activities taking place indoors such as entertainment and shopping we use the same indoor/outdoor ratios that SIREN predicts for offices and schools. For the personal exposure calculation we draw random values for indoor/outdoor ratios from the seasonal distributions. To decide whether shopping takes place indoors or outdoors we are based on statistics from the IAURIF (2006) study, following which 14% of the shopping activity in the Ile-de-France region takes place outdoors. Entertainment other than exercise is

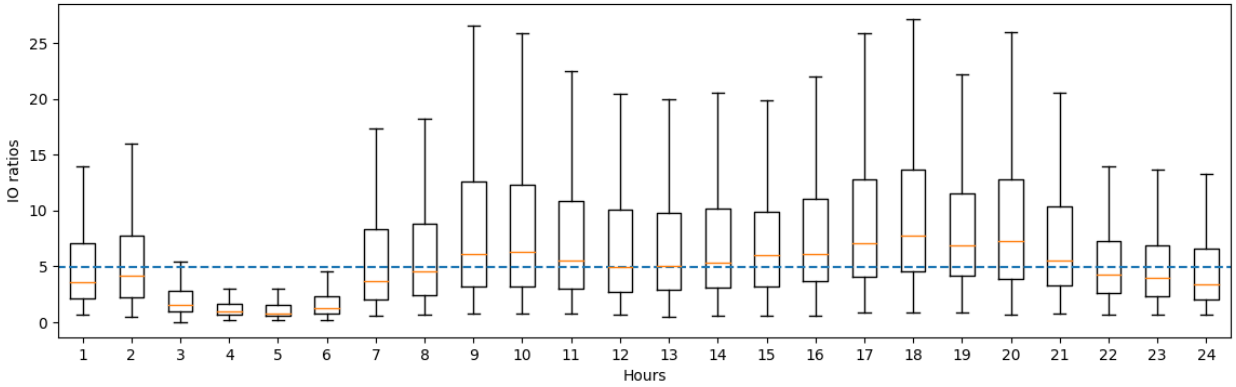

Figure 5. *Hourly distributions of indoor/outdoor $PM_{2.5}$ ratios for subway platforms issued from in-platform measurements of the SQUALES network and outdoor measurements of the AIRPARIF network. The blue line is the median I/O ratio.*

assumed to always take place indoors. For exercise activities, we first chose the type of exercise activity (IAURIF, 2006) and then whether it takes place indoors or outdoors depending on the specific activity.

4 Population data

The methodological steps to obtain activity event sequences for the sample population are listed here:

- select the population sample size that statistically reproduces essential demographics such as population of each administrative unit.
- assign attributes to the members of the population such as age, gender, principal occupation etc.
- simulate the mobility of the population by matching the journeys of the EGT (2010).

Monte-Carlo sampling method is used to randomly generate a data set of simulated individuals based on these steps.

4.1 Generation of the sample population

The population data implemented in the model are public census data published by the INSEE (Institut Nationale de la Statistique et des Études Économiques). The current version of the model implements datasets for year 2009. The administrative unit chosen for the current study is the commune. The Ile-de-France region has 1300 communes and a population of 11 726 743. The most densely populated communes are located at the outer rings of the Paris agglomeration followed by a second circle of high population density at the suburbs directly attached to the agglomeration. A third highly urbanized ring is distinguished before reaching the rural areas at the outskirts of the Ile-de-France region (Figure 6).

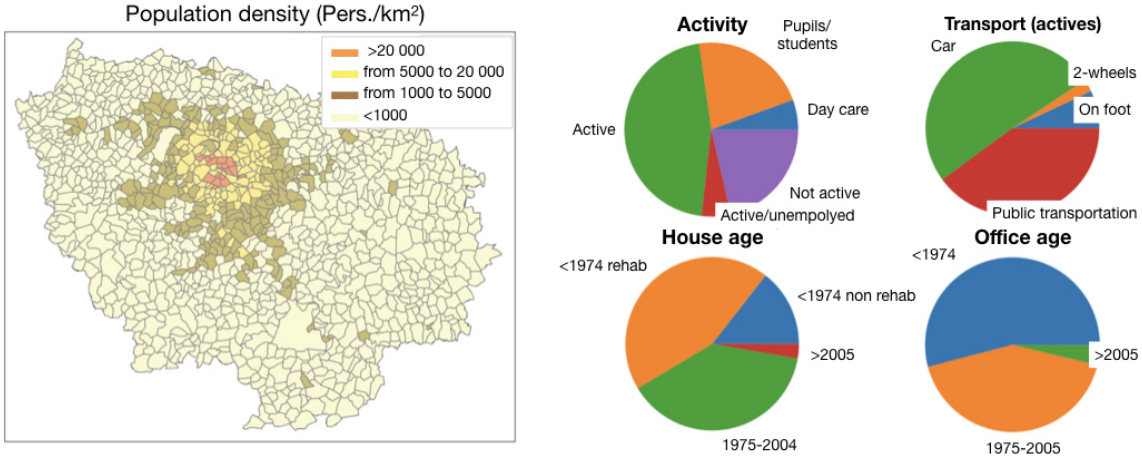

Figure 6. *Population density at the commune level in the Ile-de-France region (left). Distribution of exposure factors in the sample population (right). Data source census 2009 (INSEE).*

The size of the sample population is fixed at 250 000 individuals (≈2% of the actual population). A sensitivity analysis showed that further increasing this number does not significantly affect the results of the simulation (not shown). The first module of the model sequence assigns several demographic attributes to each member of the sample population. These attributes, referred to as exposure factors hereafter, remain unchanged throughout the simulation. The procedure consists of randomly selecting values from a distribution that matches the distribution of each attribute in the actual population of each commune. By repeating this process for each member of the sample population we are sure to reproduce the distribution of the exposure factors in the simulated population.

The population is divided in four age groups. Five occupation classes are defined, and two possible contract types (full-time or part-time) corresponding to 9-hours or 5-hours working days. Data on the construction date of the building of residence and work are also implemented, to account for the infiltration of outdoor pollution indoors. The ten exposure factors implemented in the model are listed below. The different possible values for each model parameter are shown.

- **Home commune:** 1 out of 1300
- **Gender:** Male, female
- **Age group:** <4, 4-24, 25-64, >64
- **Occupation:** Day-care, pupils/students, active employed, active unemployed, not active (retired, at home, other)
- **Contract:** No contract, full-time, part-time
- **Work area:** Same commune as residence, different commune in the same department, different commune in different Ile-de-France department, outside IdF or abroad

- **Work commune:** 1 out of 1300
- **Means of transportation:** No transportation, on foot, 2-wheels, car, public transport
- **Construction date of residence:** <1974 not rehabilitated, <1974 rehabilitated, 1974-2004, >2005
- **Construction date of work place:** <1974, 1974-2004, >2005

A certain dependency exists between the exposure factors. For example, the professional occupation strongly depends on gender and age. To preserve the sub-population variability in the sample population, the random sampling of the exposure factors operates on stratified data, where exposure factors are supposed to be homogeneous. First, we assign the commune of residence, and then the other attributes in the following order: gender, age group, principal occupation, and finally the kind of contract. Once these primary attributes assigned, we then proceed to the selection of the rest, secondary characteristics. Working area is a function of the occupation and the commune of residence, the construction date of the buildings of residence depends on the commune, the gender and the age group. For offices general statistics are provided by ADEME for each Ile-de-France department dividing offices in three age classes.

4.2 Modeling the activity sequences

The second module of the model compiles 24-hour activity event sequences for each member of the sample population. Two diaries are compiled for each individual, one for weekdays and one for weekends. At each moment in time, people are either at home, engaged in an activity, or in transport. Eligible activities are the six motives for transport in the EGT (2010), namely work, professional affairs, school, market, recreation or personal affairs. From this study, we deduce the number of journeys to take place at each hour in the region for each of the six aforementioned motives. Whenever an activity ends, or once every hour if the person is at home, the model checks whether the individual is about to move. Some restrictions are implemented, because not all individuals are eligible for all activities. For example, only certain age groups are eligible to go to day-care or school, only employed people are bound to go to work, etc. Once these restrictions are implemented, people will move in order to match the proportions of journeys per motive at each hour. If the person is bound to move, a number of choices are made in the following order: i) transportation mode ; ii) destination commune ; iii) travel distance ; iv) travel time ; v) activity duration (see also Figure 7): For journeys to work and back, the INSEE provides a detailed dataset with the principal modes of transport. This information is part of the exposure factors assigned in the previous module (Section 4.1). The only stochastic choice here is for the 2-wheels case that has a 40% and 60% share between bicycles and motorcycles respectively (EGT, 2010). For the rest of the journeys we match the proportions of the transportation modes per motive and hour from the EGT (2010).

In some cases, the destination commune is known (the person goes to work, to study, or back home). For other cases we only know whether the destination commune lies in the same department as the residence or in a different department. In this case, we first define the destination department based on data on the inter-departmental flows. Then we combine two pieces of information to assign the destination commune:

– data on the average distance travelled per means of transportation. We assume a straight line connecting the centroids of the communes. Several possible destination communes are selected based on the distance criterion.

– we use the information on the destination commune for the journeys in the EGT (2010) to assign a degree of attractiveness to the communes of the Ile-de-France region for each motive.

To assign the distance of the journey we distinguish between two cases. If the destination lies in a different commune, then the journey distance is assumed to be equal to the distance over a straight line connecting the centroids of the two communes. If the destination lies within the commune of the current location then a stochastic choice is made for the traveled distance. We use statistics for the mean distance travelled per transportation means from the residents of the different departments. Depending on the transport mode, we assign a certain range around this average value and scale the limits to the commune size (radius of a circle with an area equal to the commune's area) and randomly chose a travel distance within this range.

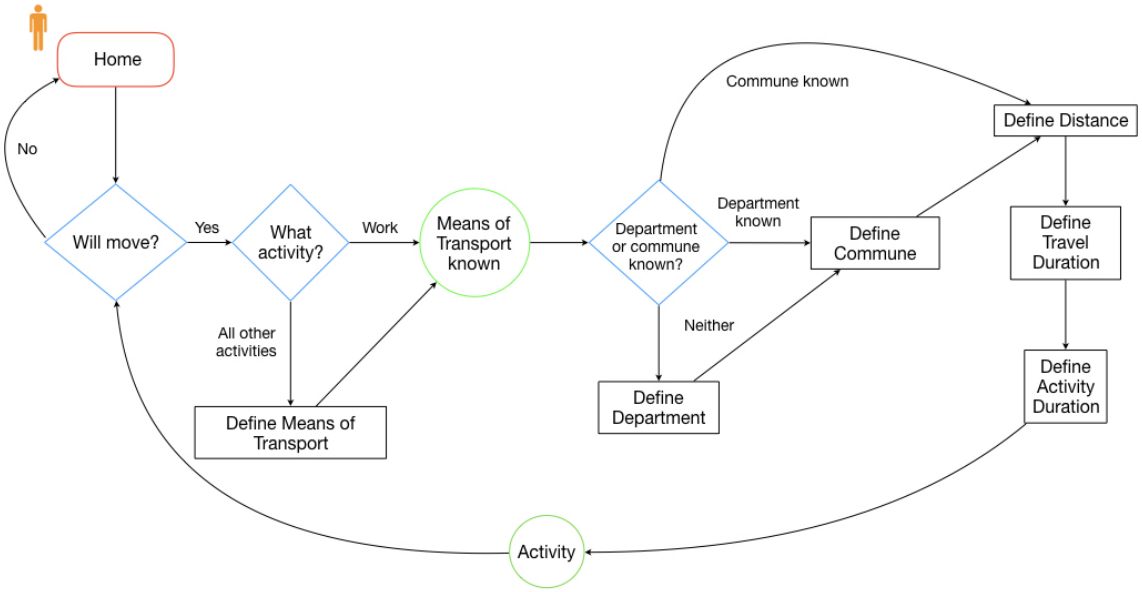

Figure 7. *Flow chart of the compilation of activity event sequences.*

To estimate the duration of the travel, we use two pieces of information at sub-communal scale. The first is the population density at 1x1km^2 resolution. Individuals are distributed over the 1x1km^2 resolution grid based on the population density. The second information is the average speed and flow over the road segments of the traffic network. We assume a straight line linking the centers of the origin and destination cells of the 1x1km^2 grid and search for all grid-cells that intersect this trajectory. The speed at which the grid cell is passed through is assigned stochastically based on the distribution of speeds over the road segments within the grid-cell. We note here that it would be more accurate to base our selection on the flows over each road segment rather than the speed distribution, but the geometry of the problem would become too complex. Given the high

resolution of the application our insight is that this simplification is not bound to introduce significant errors to the transport model. The duration of the travel is then deduced from the distance and speed.

The final step is to define the duration of the activity. For children younger than 3 years old we use statistics on the time spent at day-care. In all other cases we use statistics at department scale on the time spent by the population per activity.

A further distinction is whether the activity or transportation takes place indoors or outdoors. Certain activities may occur indoors or outdoors based on existing statistics (e.g. market and recreation). Possible means of transportation are on foot, two wheels (bicycle or motorcycle), car, bus, subway (metro), train (RER), and tramway. For public transportation, we distinguish between waiting time and travel time. For tramway, bus and RER outside Paris waiting takes place outdoors.

Figure 8 shows the results of the transport model. The diurnal patterns of the mobility of the population per motive are well reproduced. The model fails to reach the rush hour peaks, especially the morning peaks for work and school motives. It systematically underestimates the lunch hour peak. This is because the model does not implement secondary journeys i.e. people leaving the workplace to go for lunch and then back to work. These remarks become clear when looking at the total number of journeys (bottom left of Figure 8), where we also see that the model underestimates the number of journeys at all hours. However, the general picture of the simulation results is that the EGT (2010) data have been globally well implemented in the transport module.

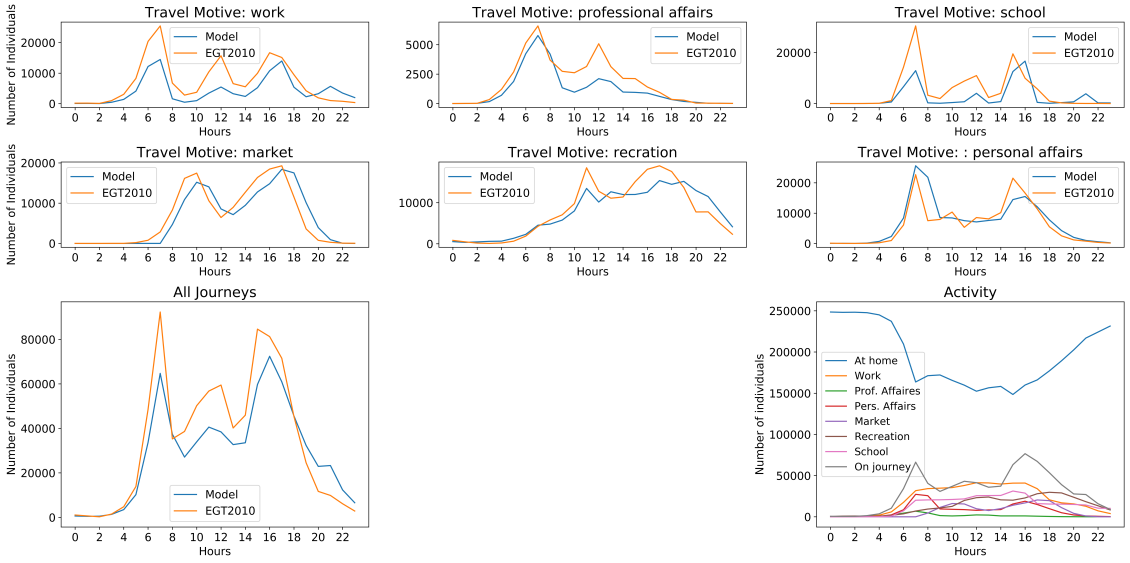

Figure 8. *Number of journeys per motive (1^{st} and 2^{nd} rows) and total number of journeys all motives included (bottom left) at each hour. The number of individuals engaged in each activity at each hour of the day.*

The transport module simulates the mobility of the population. When individuals reach their destination they engage in the activity corresponding to the journey's motive. For activities other than travel we assign a mean duration. Activity event

sequences are simulated at 1min temporal resolution. The ambient concentrations at which people are exposed during the activity is the corresponding hour-averaged concentration modeled with the CHIMERE model at the grid-cell where the activity takes place. In the case of travelling, the model simulates the trajectory of the journey. For car journeys, we use the mean hourly traffic flows on each segment of the road network to assign probabilities to each road and assign the route trajectories. The trajectory of the journey may intersect several CHIMERE grid-cells. The corresponding outdoor concentrations are weighted by the time spent in each grid-cell to estimate the aggregated exposure. Figure 8 (bottom right) shows the number of people engaged in each of the implemented activities at each hour of the simulation. Here, time-activity is modelled based on available data for the region relied on questionnaires. Modelling mobility patterns using smart phones with built-in GPS is an emerging trend in personal exposure assessment (Yu et al., 2019). Combining GPS-derived data on the trajectories of large number of individuals with information from questionnaires on the locations and activities of the population, could help overcome large part of the uncertainties relating to the time-activity module developed in this study.

5 Results

In this section we highlight different possible applications of the exposure model. Each section looks at a different aspect of the model output as exemples of its use in applications. The spatial distribution of exposure over the Ile-de-France region is discussed in Section 5.1, the relative contribution of each microenvironment in the daily aggregated exposure is quantified in Section 5.2, the variability in exposure patterns across sub-populations is studied in Section 5.3, and the impact of considering 1) the infiltration of pollutants indoors and 2) the mobility of the population is illustrated in Section 5.4. Finally, in Section 5.5 we develop a 2050 horizon projection in the building stock of the Ile-de-France region, and quantify its impact in exposure to $PM_{2.5}$ and ozone.

5.1 Exposure maps

Personal exposures may be spatially averaged over the communes to provide population exposure maps (Figure 9). The annual averaged exposure to ozone is three times higher for the residents of the remote rural areas compared to the exposure of the Parisians. NO emitted by cars over the dense road network in the Paris city reacts fast with O_3 to form NO_2. This explains the absence of O_3 over the urban agglomeration. NO_2 emitted in large amounts over Paris under the influence of sunshine and in the presence of volatile organic compounds forms O_3 downwind, over the rural area (see also Figure 3). We also note that the exposure to ozone is much lower than outdoors ozone concentration (30 and 15 ppb for the rural and urban areas respectively (compare to maps in Figure 3)). This difference is due to the high amount of time people spent indoors, where ozone concentrations are close to zero (see also I/O ratios for O_3 Figure 4).

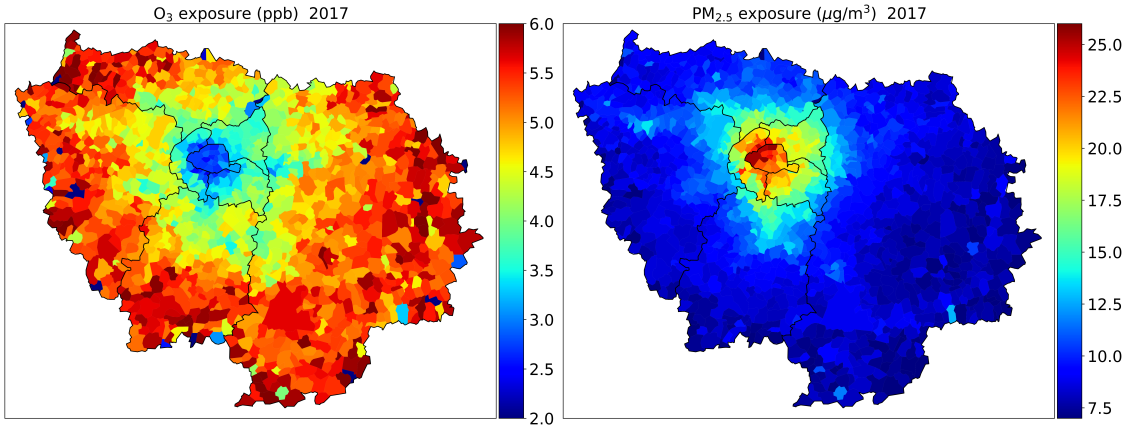

Figure 9. *Annual averaged O_3 and $PM_{2.5}$ exposure maps. Personal exposures are spatially averaged among the residents of each commune.*

The traffic network is a large source of $PM_{2.5}$, which explains why exposures to $PM_{2.5}$ are much higher in the Paris agglomeration than in the rural areas. Exposures to $PM_{2.5}$ are much closer to concentration levels because I/O ratios in buildings for $PM_{2.5}$ are closer to 1 than for O_3. Annual mean $PM_{2.5}$ concentrations are however lower than annual mean $PM_{2.5}$ exposures (compare with concentration maps in Figure 9). Even if indoor $PM_{2.5}$ sources in buildings are not yet implemented in the model and therefore concentrations in buildings are always lower than outdoor concentrations, $PM_{2.5}$ concentrations in cars, subway train or in subway platforms are several times higher than outdoor concentrations (see Table 3). Even if the time spent in transport is relatively lower than the time spent inside buildings, concentrations there are so high that the daily aggregated exposures are higher than outdoor concentrations. The construction date of buildings also plays an important role, with older buildings (higher I/O ratios) contributing to exposure at higher pollutant levels. Buildings in the Paris agglomeration are in general older than buildings outside of the city center and therefore indoor exposure to $PM_{2.5}$ is higher for the residents of Paris.

5.2 Exposure in different micro-environments

The relative contribution of exposure in different micro-environments in the aggregated daily exposure depends on outdoor concentrations, the indoor/outdoor coefficients if the activity takes place indoors, and the time spent in the micro-environment. For the active population (between 4 and 65 years old) residential exposure accounts for about 75% of daily exposure to $PM_{2.5}$ and almost 80% of the agregated exposure to O_3 (Figure 10) reflecting the large amount of time spent at home (see also bottom right panel in Figure 8). Exposure at school represents the second largest part of total daily exposure to both pollutants (more than 10%). Exposure outdoors represents a larger part of the total exposure for people between 24 and 65 years old (working

population) than for children going to school (4-23 years old). For $PM_{2.5}$ exposures in public transportation and car also have significant contributions.

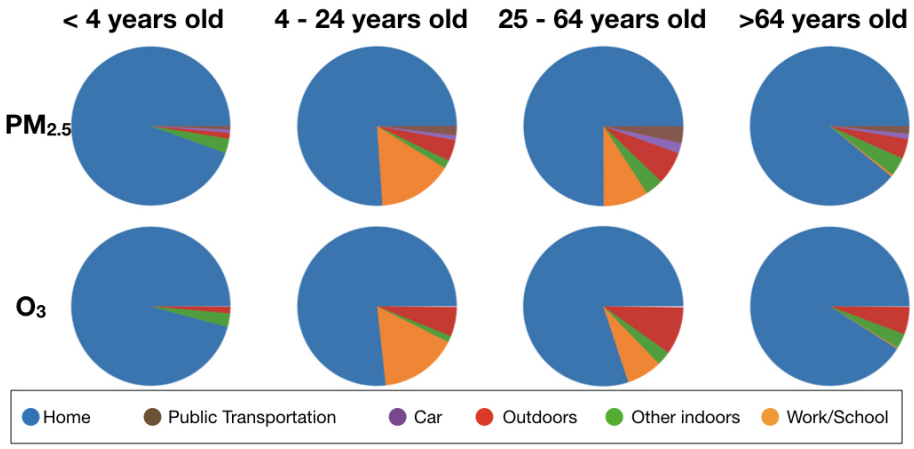

Figure 10. *Relative contribution of the different micro-environments in the aggregated daily exposures depending on the age-group.*

5.3 Exposure of sub-population groups

Here we study the impact of several exposure factors on personal exposures. Figure 11 shows the cumulative distribution of exposure over specific sub-populations. We identify the two factors that have the largest impact on personal exposures, namely the mode of transportation and the construction date of the building of residence. Both factors seem to strongly affect exposure to $PM_{2.5}$ and ozone. People traveling with motorcycles or cyces are exposed to the highest $PM_{2.5}$ levels, while exposure in cars is the lowest. 10% of the population using 2-wheels as transportation mode is exposed to $PM_{2.5}$ levels higher than the 25 $\mu g/m^3$ EU target value related to human health. The percentage of the population exposed to $PM_{2.5}$ levels above the EU target value drops to 5% for people travelling on foot, 3% for public transport and 1% for people travelling by car. The construction date of the home building also plays an important role in personal exposure. For both pollutants, exposure is higher for buildings constructed before 1974. 100% of the population living in buildings constructed after 2005 are exposed to $PM_{2.5}$ levels below the EU target value while 5% of the population living in constructions before 1974 is exposed to levels above the EU target value.

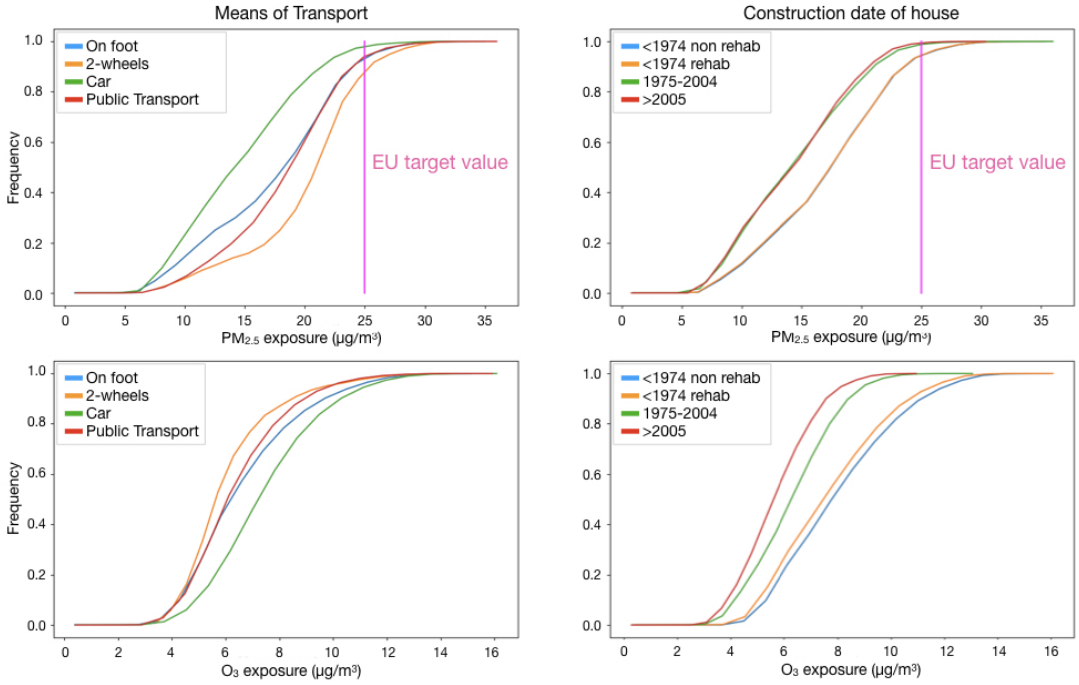

Figure 11. *Cumulative distributions of exposures to $PM_{2.5}$ (above) and O_3 (below) for sub-populations distinguished by the transportation mode (left) and construction date of the building where they live.*

5.4 Model sensitivity to population mobility and exposure indoors

Often, epidemiological methods estimate exposure metrics by modelling pollution concentrations at individual addresses. However, these models do not take into account neither exposure indoors nor population mobility. To provide insight into the exposure misclassification error due to this omission we conducted several sensitivity studies. We calculated personal exposures to $PM_{2.5}$ with and without accounting for the mobility of the population and exposure indoors as follows:

- REF The population stays at home and indoor concentrations are the same as outdoors.
- +MOBILITY The population moves but concentrations indoors are the same as outdoors.
- +INDOORS BUILDINGS The population stays at home and indoor / outdoor coefficients for buildings are applied.
- +INDOORS BUILDINGS & TRANSPORT The population moves and indoor / outdoor coefficients for both buildings and transportation are applied.

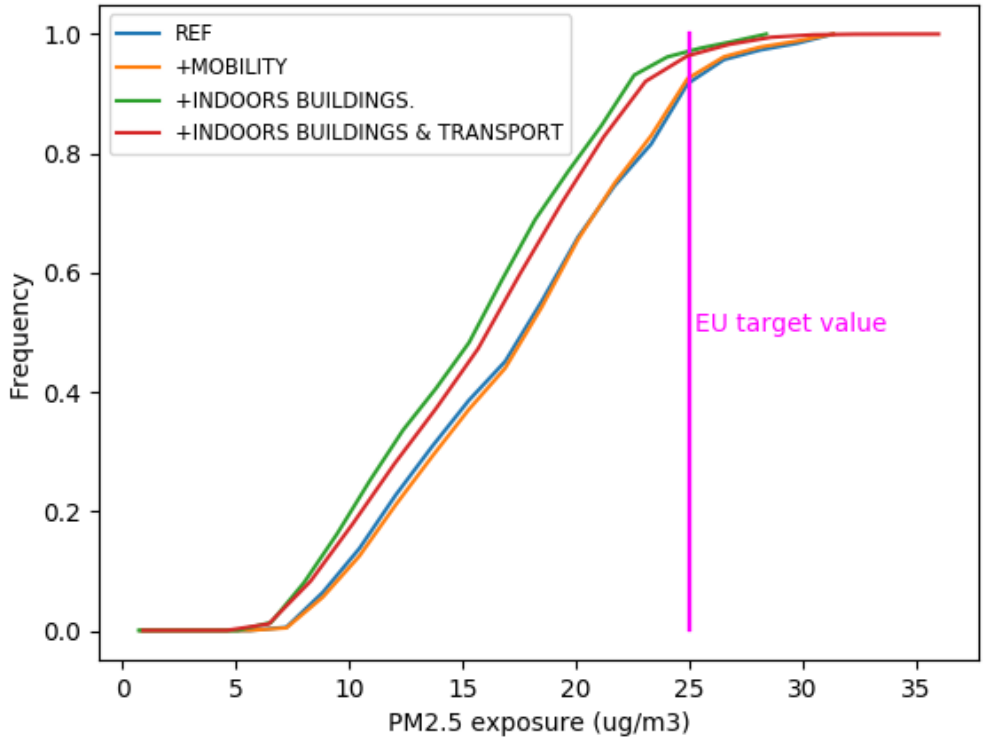

Figure 12. *Cumulative distributions of exposure to $PM_{2.5}$ resulting for simulations integrating increasing levels of complexity in the input data*

Comparing the REF simulation with +MOBILITY shows that the mobility of the population within the region alone has a small negative impact on personal exposures (-1.5% on the median). This may be explained by the fact that people spend most of their time indoors. We note here, that Shekarrizfard et al. (2016) found an increase in personal exposures to NO_2 that may be as high as +10% in the Montreal metropolitan area when population mobility was accounted for compared to the simpler set-up where exposure at individual address was considered. This is explained by the difference in the air-quality models used in each study: a gaussian dispersion model around each segment of the road network for the Shekarrizfard et al. (2016) study compared to a regional scale CTM in our case. Accounting for residential exposure in the +INDOORS BUILDINGS simulation strongly affects personal exposures (-11% difference with the REF in the median exposure). Accounting also for indoors exposure during transportation +INDOORS BUILDINGS & TRANSPORT leads to a 4.6% increase in the median exposure compared to only accounting for residential exposures (+INDOORS BUILDINGS). $PM_{2.5}$ concentrations during transportation are higher than outdoors whereas concentrations in buildings are always lower than outdoors (no indoor sources in buildings). These results are comparable to the findings of Smith et al. (2016) who also estimate a decrease in personal

exposures to $PM_{2.5}$ in the London metropolitan area when population mobility and indoor exposure are accounted for. In the REF simulation 5% of the population is exposed to concentrations above the EU target value of 25μg/m^3 while in the complete implementation of indoor exposures only 2% of the population is exposed to $PM_{2.5}$ above this threshold (Figure 12).

5.5 2050 horizon projection of the building stock

Based on data on the evolution of the French building stock (INSEE, 2014) and the national thermal building regulation found in the 2013 report of the Agence de l'Environnement et de la Maitrise de l'Energie (ADEME, 2013), the CSTB developed a projection for the evolution of the building stock that is applied here for the 2050 horizon. To comply with thermal legislations and energy demand, buildings will tend to be more air-tight and ventilation systems more efficient. This evolution in the building stock will also affect air-quality in buildings, and therefore human exposure to atmospheric contaminants.

Following this projection, in 2050 dwellings, offices and schools will still fall in the same categories presented in Table 2 but the proportions of buildings falling in each category will change due to demolition, new construction and thermal rehabilitation. The projection developed here models the annual rate of change in the building stock as follows:

For dwellings (Equation 3):

- Buildings belonging to the 5^{th} class (construction date >2012) will increase
- Buildings belonging in the 1^{st} class (<1974 not rehabilitated) will decrease due to demolition and thermal rehabilitation
- Buildings belonging to the 2^{nd} class (<1974 rehabilitated) will increase due to thermal rehabilitation of buildings in the 1^{st} class

$$
\begin{aligned}
N_{D5}^{n+1} &= N_{D5}^{n} + 0.012 * \sum_{1}^{5} N_{Di}^{n} \\
N_{D1}^{n+1} &= N_{D1}^{n} - 0.01 * \sum_{1}^{5} N_{Di}^{n} \\
N_{D1}^{n+1} &= N_{D1}^{n} - 0.015 * \sum_{1}^{5} N_{Di}^{n} \\
N_{D2}^{n+1} &= N_{D2}^{n} + 0.015 * \sum_{1}^{5} N_{Di}^{n}
\end{aligned}
\tag{3}
$$

For offices and schools (Equation 4):

- Buildings belonging to the 3^{rd} class (2006-2012) will increase
- Buildings belonging to the 1^{st} class (<1974 not rehabilitated) will decrease due to demolition

$$N_{B1}^{n+1} = N_{B1}^{n} - 0.03 * \sum_{1}^{3} N_{Bi}^{n}$$
$$N_{B3}^{n+1} = N_{B3}^{n} + 0.03 * \sum_{1}^{3} N_{Bi}^{n} \quad (4)$$

The projection is applied to the Ile-de-France building stock, and we simulate personal exposures to quantify its impact. Due to new buildings being more air-tight with a better control of air renewal using more efficient ventilation systems, even less ozone penetrates the building shell. The resulting reduction in annual average exposure to O_3 is up to 14% (Figure 13). The change in annual averaged $PM_{2.5}$ exposure is very small (not shown).

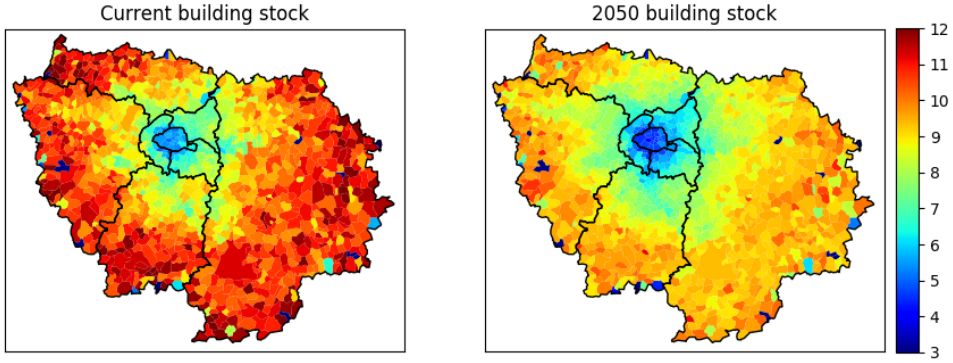

Figure 13. *Exposure to O_3 ($\mu g/m^3$) considering the actual building stock (left) and the 2050 horizon projection of the building stock (right).*

6 Conclusions

We developed a regional scale model for personal exposures to $PM_{2.5}$ and O_3. The model uses simulated outdoor pollutant concentrations and models the infiltration of outdoor contaminants indoors in buildings with a ventilation mass-balance model. Three building types are considered: dwellings, schools and offices. It also models population mobility inside the region considering the different possible transportation modes and adjusts for pollutant concentrations inside cars, buses, tram, subway train and regional trains. A special treatment for concentrations in subway platforms is applied considering online measurements on the platform and outdoors. An adjustment for ambient concentrations inside road-tunnels is also applied from data

from the literature. The model also uses data from the road traffic network to estimate the most probable trajectory for travel, as well as mean travel speed and duration.

We show that considering the population daily movement inside the region without accounting for the penetration of outdoor pollution indoors or indoor concentration during transportation has a small negative impact on annual averaged personal exposures. This is in contrast with the previous study of Shekarrizfard et al. (2016) who found an increase in exposures to NO_2 in the Montreal metropolitan area when population mobility is accounted for. However, the two models are not directly comparable since they look at different pollutants, at different time-scales and use different air-quality models.

We show that, accounting for the penetration of outdoor pollution indoors in buildings without considering population movement decreases annual averaged personal exposures by 11% for $PM_{2.5}$. This decrease stems only from the buildings' envelope acting as barrier to pollution infiltration indoors. When accounting also for population movement, annual averaged population exposures increase by 5%, showing the importance of exposure during transportation. Even if travelling represents only a small portion of time, exposures to $PM_{2.5}$ are too high and increase the daily burden of exposure. These results are in alignment with the previous study of Smith et al. (2016) who also found that personal exposures decrease in London when population mobility and exposure indoors are taken into account. The discrepancy in the magnitude of the decrease (-37% in their case vs. -7% in ours) may be due to the relatively coarse resolution of the outdoor concentration fields simulated with CHIMERE (2km x 2km). However, if this resolution is not enough to solve concentration gradients at the proximity of local sources such as roads, it is capable to distinguish between urban, suburban and rural concentrations. Most of the daily movement in the region crosses these boundaries (e.g. people living at the suburbs work in Paris and vice-versa).

We conclude that both infiltration of pollutant indoors and population movement need to be considered to estimate the aggregated daily exposure. We note here that, so far, the model does not implement indoor sources of $PM_{2.5}$ in buildings. We are aware that $PM_{2.5}$ indoors may be several times higher than outdoor concentrations (as is the case during transport). However, in this version of the model we were more interested to see how different building types and characteristics affect personal exposures independent of human activity that would drive indoor sources. The CSTB is working actively to develop parametrizations accounting for indoor emission sources of $PM_{2.5}$ as well as their resuspension due to human activity.

Several applications of the model are presented. We first show the maps of exposure to O_3 and $PM_{2.5}$ over the region. The spatial distribution of the exposure field is very similar to the concentration one, showing the strong correlation of the aggregated exposure to outdoor concentration. However, we show that if we focus on specific sub-population groups, such as people using bicycles or motorcycles systematically in their daily journeys or people living in houses built before 1974, the upper percentiles of exposure are much higher than the general population. To study the impact of buildings' characteristics on personal exposures we implemented a 2050-horizon projection of the building stock in the Ile-de-France region. Following this projection, older buildings will be demolished or rehabilitated to comply with the thermal regulation and newer constructions will have modernized characteristics. The share of people living in the different building categories is modified to match this projection and personal exposures are simulated. 2050-horizon personal exposures to O_3 are decreased by as much as 14% according to this projection.

This first version of the model is parametrized for data available for greater Paris. However, the input data required for the simulation are also possible to find in other regions: census data, construction dates of buildings, mobility data. We can therefore imagine that with small adjustments in the format, the model could be applied to other regions. In all applications presented here, outdoor concentration data are simulated with the CHIMERE model and therefore the horizontal resolution is limited to the order of 1km x 1km. However, this resolution limit is not inherent for the exposure model. If outdoor concentration fields at higher horizontal resolution were available from another dispersion model (e.g Gaussian or Lagrangian), the exposure calculation would have run without any modification being necessary.

Code and data availability. The source code of the EXPLUME v1.0 model, as well as all necessary input data for the Ile-de-France region (open source see acknowledgements) are available under the doi:10.5281/zenodo.3352713

Competing interests. The authors declare that they have no conflict of interest.

Acknowledgement. This work has received funding from the European Union's Horizon 2020 research and innovation program under the grant agreement PULSE No. 727816 as well as from ANSES, ADEME, BelSPO, UBA and the Swedish EPA under the ERA-ENVHEALTH network grant agreement ACCEPTED no. 219337. This work was performed using HPC resources from GENCI TGCC under grant No. A0050110274. The authors acknowledge AIRPARIF for developing and providing the bottom-up anthropogenic emissions inventory used in this study. We also acknowledge RATP for maintaining the SQUALES network and publishing the data as well as STIF, OMNIL and DRIEA for rendering public the EGT2010 dataset. Finally, we acknowledge Raphael Lachieze Rey for his valuable help in the statistical modeling.

References

ADEME: Les chiffres clés du bâtiment: énergie-environnement, Tech. Rep. Chiffes clés, Agence de l'Environnement et de la Maitrise de l'Energie, 2013.

AIRPARIF: Quelle qualité de l'air en voiture pendant les trajets quotidiens domicile-travail, Tech. rep., AIRPARIF, https://www.airparif.asso.fr/_pdf/publications/synthese_expovoituredomtra.pdf, https://www.airparif.asso.fr/_pdf/publications/synthese_expovoituredomtra.pdf, 2009.

Anderson, H. R., Atkinson, R. W., Peacock, J., Marston, L., and Konstantinou, K.: Meta-analysis of time-series studies and panel studies of particulate matter (PM) and ozone (O3) : report of a WHO task group, https://apps.who.int/iris/handle/10665/107557, 2004.

Atkinson, R. W., Mills, I. C., Walton, H. A., and Anderson, H. R.: Fine particle components and health—a systematic review and meta-analysis of epidemiological time series studies of daily mortality and hospital admissions, Journal of Exposure Science & Environmental Epidemiology, 25, 208–214, https://doi.org/10.1038/jes.2014.63, https://www.ncbi.nlm.nih.gov/pmc/articles/PMC4335916/, 2015.

Batterman, S., Ganguly, R., Isakov, V., Burke, J., Arunachalam, S., Snyder, M., Robins, T., and Lewis, T.: Dispersion Modeling of Traffic-Related Air Pollutant Exposures and Health Effects Among Children with Asthma in Detroit, Michigan, Transportation Research Record, 2452, 105–112, https://doi.org/10.3141/2452-13, 2014.

Beauchamp, M., Malherbe, L., and de Fouquet, C.: A pragmatic approach to estimate the number of days in exceedance of PM10 limit value, Atmospheric Environment, 111, 79–93, https://doi.org/10.1016/j.atmosenv.2015.03.062, http://www.sciencedirect.com/science/article/pii/S1352231015002861, 2015.

Beelen, R., Hoek, G., Vienneau, D., Eeftens, M., Dimakopoulou, K., Pedeli, X., Tsai, M.-Y., Künzli, N., Schikowski, T., Marcon, A., Eriksen, K. T., Raaschou-Nielsen, O., Stephanou, E., Patelarou, E., Lanki, T., Yli-Tuomi, T., Declercq, C., Falq, G., Stempfelet, M., Birk, M., Cyrys, J., von Klot, S., Nádor, G., Varró, M. J., Dėdelė, A., Gražulevičienė, R., Mölter, A., Lindley, S., Madsen, C., Cesaroni, G., Ranzi, A., Badaloni, C., Hoffmann, B., Nonnemacher, M., Krämer, U., Kuhlbusch, T., Cirach, M., de Nazelle, A., Nieuwenhuijsen, M., Bellander, T., Korek, M., Olsson, D., Strömgren, M., Dons, E., Jerrett, M., Fischer, P., Wang, M., Brunekreef, B., and de Hoogh, K.: Development of NO2 and NOx land use regression models for estimating air pollution exposure in 36 study areas in Europe – The ESCAPE project, Atmospheric Environment, 72, 10–23, https://doi.org/10.1016/j.atmosenv.2013.02.037, http://www.sciencedirect.com/science/article/pii/S1352231013001386, 2013.

Beevers, S. D., Kitwiroon, N., Williams, M. L., Kelly, F. J., Ross Anderson, H., and Carslaw, D. C.: Air pollution dispersion models for human exposure predictions in London, Journal of Exposure Science & Environmental Epidemiology, 23, 647–653, https://doi.org/10.1038/jes.2013.6, 2013.

Bell, M. L., Dominici, F., and Samet, J. M.: A meta-analysis of time-series studies of ozone and mortality with comparison to the national morbidity, mortality, and air pollution study, Epidemiology (Cambridge, Mass.), 16, 436–445, http://www.ncbi.nlm.nih.gov/pubmed/15951661, 2005.

Berchet, A., Zink, K., Muller, C., Oettl, D., Brunner, J., Emmenegger, L., and Brunner, D.: A cost-effective method for simulating city-wide air flow and pollutant dispersion at building resolving scale, Atmospheric Environment, 158, 181–196, https://doi.org/10.1016/j.atmosenv.2017.03.030, http://www.sciencedirect.com/science/article/pii/S1352231017301620, 2017.

Blair, A., Stewart, P., Lubin, J. H., and Forastiere, F.: Methodological issues regarding confounding and exposure misclassification in epidemiological studies of occupational exposures, https://doi.org/10.1002/ajim.20281, https://onlinelibrary.wiley.com/doi/abs/10.1002/ajim.20281, 2007.

Cassee, F. R., Héroux, M.-E., Gerlofs-Nijland, M. E., and Kelly, F. J.: Particulate matter beyond mass: recent health evidence on the role of fractions, chemical constituents and sources of emission, Inhalation Toxicology, 25, 802–812, https://doi.org/10.3109/08958378.2013.850127, https://www.ncbi.nlm.nih.gov/pmc/articles/PMC3886392/, 2013.

Cattani, G., Gaeta, A., Di Menno di Bucchianico, A., De Santis, A., Gaddi, R., Cusano, M., Ancona, C., Badaloni, C., Forastiere, F., Gariazzo, C., Sozzi, R., Inglessis, M., Silibello, C., Salvatori, E., Manes, F., and Cesaroni, G.: Development of land-use regression models for exposure assessment to ultrafine particles in Rome, Italy, Atmospheric Environment, 156, 52–60, https://doi.org/10.1016/j.atmosenv.2017.02.028, http://www.sciencedirect.com/science/article/pii/S1352231017301085, 2017.

Chen, C. and Zhao, B.: Review of relationship between indoor and outdoor particles: I/O ratio, infiltration factor and penetration factor, Atmospheric Environment, 45, 275–288, https://doi.org/10.1016/j.atmosenv.2010.09.048, http://www.sciencedirect.com/science/article/pii/S1352231010008241, 2011.

Collignan, B., Lorkowski, C., and Améon, R.: Development of a methodology to characterize radon entry in dwellings, Building and Environment, 57, 176–183, https://doi.org/10.1016/j.buildenv.2012.05.002, http://www.sciencedirect.com/science/article/pii/S0360132312001503, 2012.

Cyrys, J., Pitz, M., Bischof, W., Wichmann, H.-E., and Heinrich, J.: Relationship between indoor and outdoor levels of fine particle mass, particle number concentrations and black smoke under different ventilation conditions, Journal of Exposure Science & Environmental Epidemiology, 14, 275, https://doi.org/10.1038/sj.jea.7500317, https://www.nature.com/articles/7500317, 2004.

Delaunay C., Goupil G., Ravelomanantsoa H., Person A., Mazoue S., and Morawski F.: City dwellers exposure to atmospheric pollutants when commuting in Paris urban area., 2012.

Di, Q., Wang, Y., Zanobetti, A., Wang, Y., Koutrakis, P., Choirat, C., Dominici, F., and Schwartz, J. D.: Air Pollution and Mortality in the Medicare Population, New England Journal of Medicine, 376, 2513–2522, https://doi.org/10.1056/NEJMoa1702747, https://doi.org/10.1056/NEJMoa1702747, 2017.

Dias, D. and Tchepel, O.: Spatial and Temporal Dynamics in Air Pollution Exposure Assessment, International Journal of Environmental Research and Public Health, 15, 558, https://doi.org/10.3390/ijerph15030558, https://www.mdpi.com/1660-4601/15/3/558, 2018.

Edwards, J. K. and Keil, A. P.: Measurement Error and Environmental Epidemiology: A Policy Perspective, Current environmental health reports, 4, 79–88, https://doi.org/10.1007/s40572-017-0125-4, https://www.ncbi.nlm.nih.gov/pmc/articles/PMC5374270/, 2017.

EEA: Air quality in Europe — 2019, Tech. Rep. 10/2019, https://www.eea.europa.eu//publications/air-quality-in-europe-2019, 2019.

EGT: Enquête Globale Transport 2010-STIF-OMNIL-DRIEA, Tech. rep., 2010.

Franklin, M., Vora, H., Avol, E., McConnell, R., Lurmann, F., Liu, F., Penfold, B., Berhane, K., Gilliland, F., and Gauderman, W. J.: Predictors of intra-community variation in air quality, Journal of Exposure Science and Environmental Epidemiology, 22, 135–147, https://doi.org/10.1038/jes.2011.45, https://www.nature.com/articles/jes201145, 2012.

Georgopoulos, P. G., Wang, S.-W., Vyas, V. M., Sun, Q., Burke, J., Vedantham, R., McCurdy, T., and Ozkaynak, H.: A source-to-dose assessment of population exposures to fine PM and ozone in Philadelphia, PA, during a summer 1999 episode, J Expo Anal Environ Epidemiol, 15, 439–457, http://dx.doi.org/10.1038/sj.jea.7500422, 2005.

HEI: Traffic-Related Air Pollution: A Critical Review of the Literature on Emissions, Exposure, and Health Effects, Tech. Rep. Special Report 17, Health Effects Institute, Boston, MA, https://www.healtheffects.org/publication/traffic-related-air-pollution-critical-review-literature-emissions-exposure-and-health, 2010.

Hodas, N., Meng, Q., Lunden, M. M., Rich, D. Q., Özkaynak, H., Baxter, L. K., Zhang, Q., and Turpin, B. J.: Variability in the fraction of ambient fine particulate matter found indoors and observed heterogeneity in health effect estimates, Journal of Exposure Science and Environmental Epidemiology, 22, 448–454, https://doi.org/10.1038/jes.2012.34, https://www.nature.com/articles/jes201234, 2012.

Hwang, Y. and Lee, K.: Contribution of microenvironments to personal exposures to PM10 and PM2.5 in summer and winter, Atmospheric Environment, 175, 192–198, https://doi.org/10.1016/j.atmosenv.2017.12.009, http://www.sciencedirect.com/science/article/pii/S1352231017308269, 2018.

IAURIF: Les déplacements pour achats. Analyse des comportements des franciliens en matière de déplacements pour achats, Tech. Rep. Delaporte C, Courel J., Les cahiers de l'Enquête Globale de Transport. No 7., 2006.

INSEE: Tableaux de l'économie francaise, Tech. rep., Institut Nationale de la statistique et des études économiques, Editions INSEE, 2014.

J., W. C.: Ozone in Indoor Environments: Concentration and Chemistry, Indoor Air, 10, 269–288, https://doi.org/10.1034/j.1600-0668.2000.010004269.x, https://onlinelibrary.wiley.com/doi/full/10.1034/j.1600-0668.2000.010004269.x, 2000.

K. Wyat Appel, Robert C. Gilliam, Jonathan E. Pleim, George A. Pouliot, David C. Wong, Christian Hogrefe, Shawn J. Roselle, and Rohit Mathur: Improvements to the WRF-CMAQ modeling system for fine-scale air quality simulations, EM: AIR AND WASTE MANAGEMENT ASSOCIATION'S MAGAZINE FOR ENVIRONMENTAL MANAGERS, pp. 16–21, https://cfpub.epa.gov/si/si_public_record_report.cfm?Lab=NERL&dirEntryId=288280, 2014.

Klepeis, N. E.: Synopsis, 2006.

Korek, M. J., Bellander, T. D., Lind, T., Bottai, M., Eneroth, K. M., Caracciolo, B., Faire, U. H. d., Fratiglioni, L., Hilding, A., Leander, K., Magnusson, P. K. E., Pedersen, N. L., Östenson, C.-G., Pershagen, G., and Penell, J. C.: Traffic-related air pollution exposure and incidence of stroke in four cohorts from Stockholm, Journal of Exposure Science & Environmental Epidemiology, 25, 517–523, https://doi.org/10.1038/jes.2015.22, https://www.nature.com/articles/jes201522, 2015.

L. Morawska, C. He: Relationship between indoor/outdoor concentrations of particles: a critical review, in: Proceedings of the 7th International Conference Healthy Buildings, pp. 7–11, National University of Singapore, Singapore, 2003.

Lim, S., Kim, J., Kim, T., Lee, K., Yang, W., Jun, S., and Yu, S.: Personal exposures to PM2.5 and their relationships with microenvironmental concentrations, Atmospheric Environment, 47, 407–412, https://doi.org/10.1016/j.atmosenv.2011.10.043, http://www.sciencedirect.com/science/article/pii/S1352231011011228, 2012.

Lipfert, F. W. and Wyzga, R. E.: On exposure and response relationships for health effects associated with exposure to vehicular traffic, Journal of Exposure Science and Environmental Epidemiology, 18, 588–599, https://doi.org/10.1038/jes.2008.4, https://www.nature.com/articles/jes20084, 2008.

Mailler, S., Menut, L., Khvorostyanov, D., Valari, M., Couvidat, F., Siour, G., Turquety, S., Briant, R., Tuccella, P., Bessagnet, B., Colette, A., Létinois, L., Markakis, K., and Meleux, F.: CHIMERE-2017: from urban to hemispheric chemistry-transport modeling, Geoscientific Model Development, 10, 2397–2423, https://doi.org/https://doi.org/10.5194/gmd-10-2397-2017, https://www.geosci-model-dev.net/10/2397/2017/, 2017.

Matson, U.: Indoor and outdoor concentrations of ultrafine particles in some Scandinavian rural and urban areas, Science of The Total Environment, 343, 169–176, https://doi.org/10.1016/j.scitotenv.2004.10.002, http://www.sciencedirect.com/science/article/pii/S0048969704007004, 2005.

McBride, S. J., Williams, R. W., and Creason, J.: Bayesian hierarchical modeling of personal exposure to particulate matter, Atmospheric Environment, 41, 6143–6155, https://doi.org/10.1016/j.atmosenv.2007.04.005, http://www.sciencedirect.com/science/article/pii/S1352231007003408, 2007.

Miranda, M. L., Edwards, S. E., Chang, H. H., and Auten, R. L.: Proximity to roadways and pregnancy outcomes, Journal of Exposure Science & Environmental Epidemiology, 23, 32–38, https://doi.org/10.1038/jes.2012.78, 2013.

Monn, C.: Exposure assessment of air pollutants: a review on spatial heterogeneity and indoor/outdoor/personal exposure to suspended particulate matter, nitrogen dioxide and ozone, Atmospheric Environment, 35, 1–32, https://doi.org/10.1016/S1352-2310(00)00330-7, http://www.sciencedirect.com/science/article/pii/S1352231000003307, 2001.

Morales Betancourt, R., Galvis, B., Rincón-Riveros, J. M., Rincón-Caro, M. A., Rodriguez-Valencia, A., and Sarmiento, O. L.: Personal exposure to air pollutants in a Bus Rapid Transit System: Impact of fleet age and emission standard, Atmospheric Environment, 202, 117–127, https://doi.org/10.1016/j.atmosenv.2019.01.026, http://www.sciencedirect.com/science/article/pii/S1352231019300482, 2019.

Olsson, D., Bråbäck, L., and Forsberg, B.: Air pollution exposure during pregnancy and infancy and childhood asthma, European Respiratory Journal, 44, P4237, https://erj.ersjournals.com/content/44/Suppl_58/P4237, 2014.

Olstrup, H., Johansson, C., Forsberg, B., Tornevi, A., Ekebom, A., and Meister, K.: A Multi-Pollutant Air Quality Health Index (AQHI) Based on Short-Term Respiratory Effects in Stockholm, Sweden, International Journal of Environmental Research and Public Health, 16, https://doi.org/10.3390/ijerph16010105, 2019a.

Olstrup, H., Johansson, C., Forsberg, B., and Åström, C.: Association between Mortality and Short-Term Exposure to Particles, Ozone and Nitrogen Dioxide in Stockholm, Sweden, International Journal of Environmental Research and Public Health, 16, https://doi.org/10.3390/ijerph16061028, 2019b.

OQAI: Campagne nationale Logements Etat de la qualité de l'air dans les gogements francais Rapport final, Tech. Rep. DDD/SB – 2006-57, Observatoire de la qualité de l'air interieur, Kirchner S, Arenes J-F, Cochet C, Derbez M, Duboudin C, Elias P, Gregoire A., Jédor B., Lucas J-P, Pasquier N., Pigneret M., Ramalho O, 2006.

Orru H, B. Lövenheim, C. Johansson, B. Forsberg: Health impacts of traffic exhaust in road tunnels – a case of planned 18 km long high-way road tunnel by-pass in Stockholm, Umea, 2015.

Pascal, M., Corso, M., Chanel, O., Declercq, C., Badaloni, C., Cesaroni, G., Henschel, S., Meister, K., Haluza, D., Martin-Olmedo, P., and Medina, S.: Assessing the public health impacts of urban air pollution in 25 European cities: Results of the Aphekom project, Science of The Total Environment, 449, 390–400, https://doi.org/10.1016/j.scitotenv.2013.01.077, http://www.sciencedirect.com/science/article/pii/S0048969713001320, 2013.

Pascal, M., de Crouy Chanel, P., Wagner, V., Corso, M., Tillier, C., Bentayeb, M., Blanchard, M., Cochet, A., Pascal, L., Host, S., Goria, S., Le Tertre, A., Chatignoux, E., Ung, A., Beaudeau, P., and Medina, S.: The mortality impacts of fine particles in France, Science of The Total Environment, 571, 416–425, https://doi.org/10.1016/j.scitotenv.2016.06.213, http://www.sciencedirect.com/science/article/pii/S0048969716314024, 2016.

Ryan, P. H. and LeMasters, G. K.: A review of land-use regression models for characterizing intraurban air pollution exposure, Inhalation Toxicology, 19 Suppl 1, 127–133, https://doi.org/10.1080/08958370701495998, 2007.

Sarnat, J. A., Wilson, W. E., Strand, M., Brook, J., Wyzga, R., and Lumley, T.: Panel discussion review: session 1–exposure assessment and related errors in air pollution epidemiologic studies, Journal of Exposure Science & Environmental Epidemiology, 17 Suppl 2, S75–82, https://doi.org/10.1038/sj.jes.7500621, http://www.ncbi.nlm.nih.gov/pubmed/18079768, 2007.

Shekarrizfard, M., Faghih-Imani, A., and Hatzopoulou, M.: An examination of population exposure to traffic related air pollution: Comparing spatially and temporally resolved estimates against long-term average exposures at the home location, Environmental Research, 147, 435–444, https://doi.org/10.1016/j.envres.2016.02.039, http://www.sciencedirect.com/science/article/pii/S0013935116300809, 2016.

Skamarock, C., Klemp, B., Dudhia, J., Gill, O., Barker, D., Duda, G., Huang, X.-y., Wang, W., and Powers, G.: A Description of the Advanced Research WRF Version 3, https://doi.org/10.5065/D68S4MVH, https://opensky.ucar.edu:/islandora/object/technotes%3A500/, 2008.

Smith, J. D., Mitsakou, C., Kitwiroon, N., Barratt, B. M., Walton, H. A., Taylor, J. G., Anderson, H. R., Kelly, F. J., and Beevers, S. D.: London Hybrid Exposure Model: Improving Human Exposure Estimates to NO2 and PM2.5 in an Urban Setting, Environmental Science & Technology, 50, 11 760–11 768, https://doi.org/10.1021/acs.est.6b01817, https://doi.org/10.1021/acs.est.6b01817, 2016.

Soares, J., Kousa, A., Kukkonen, J., Matilainen, L., Kangas, L., Kauhaniemi, M., Riikonen, K., Jalkanen, J.-P., Rasila, T., Hänninen, O., Koskentalo, T., Aarnio, M., Hendriks, C., and Karppinen, A.: Refinement of a model for evaluating the population exposure in an urban area, Geoscientific Model Development, 7, 1855–1872, https://doi.org/https://doi.org/10.5194/gmd-7-1855-2014, https://www.geosci-model-dev.net/7/1855/2014/, 2014.

Stephens, B., Gall, E. T., and Siegel, J. A.: Measuring the penetration of ambient ozone into residential buildings, Environmental Science & Technology, 46, 929–936, https://doi.org/10.1021/es2028795, 2012.

Sun, Q., Wang, W., Chen, C., Ban, J., Xu, D., Zhu, P., He, M. Z., and Li, T.: Acute effect of multiple ozone metrics on mortality by season in 34 Chinese counties in 2013–2015, Journal of Internal Medicine, 283, 481–488, https://doi.org/10.1111/joim.12724, https://onlinelibrary.wiley.com/doi/abs/10.1111/joim.12724, 2018.

Thatcher, T. L., Lunden, M. M., Revzan, K. L., Sextro, R. G., and Brown, N. J.: A Concentration Rebound Method for Measuring Particle Penetration and Deposition in the Indoor Environment, Aerosol Science and Technology, 37, 847–864, https://doi.org/10.1080/02786820300940, https://doi.org/10.1080/02786820300940, 2003.

Valari, M. and Menut, L.: Transferring the heterogeneity of surface emissions to variability in pollutant concentrations over urban areas through a chemistry-transport model, Atmospheric Environment, 44, 3229–3238, https://doi.org/10.1016/j.atmosenv.2010.06.001, http://www.sciencedirect.com/science/article/B6VH3-5093N9B-6/2/2372afd4aad530a0eea42d4c5bb8e4d7, 2010.

Valari, M., Menut, L., and Chatignoux, E.: Using a chemistry transport model to account for the spatial variability of exposure concentrations in epidemiologic air pollution studies, Journal of the Air & Waste Management Association (1995), 61, 164–179, 2011.

Vizcaino, P. and Lavalle, C.: Development of European NO2 Land Use Regression Model for present and future exposure assessment: Implications for policy analysis, Environmental Pollution, 240, 140–154, https://doi.org/10.1016/j.envpol.2018.03.075, http://www.sciencedirect.com/science/article/pii/S0269749117348674, 2018.

Walker, I., Sherman, M., and Nazaroff, W.: Ozone Reductions Using Residential Building Envelopes, Tech. Rep. LBNL-1563E, Lawrence Berkeley National Laboratory, california Institute for Energy and Environment, 2009.

Walker, I. S. and Sherman, M. H.: Effect of ventilation strategies on residential ozone levels, Building and Environment, 59, 456–465, https://doi.org/10.1016/j.buildenv.2012.09.013, http://www.sciencedirect.com/science/article/pii/S0360132312002557, 2013.

WHO: Burden of Disease from Ambient Air Pollution for 2012, 2014.

Willers, S. M., Eriksson, C., Gidhagen, L., Nilsson, M. E., Pershagen, G., and Bellander, T.: Fine and coarse particulate air pollution in relation to respiratory health in Sweden, European Respiratory Journal, 42, 924–934, https://doi.org/10.1183/09031936.00088212, https://erj.ersjournals.com/content/42/4/924, 2013.

Williams, R. D. and Knibbs, L. D.: Daily personal exposure to black carbon: A pilot study, Atmospheric Environment, 132, 296–299, https://doi.org/10.1016/j.atmosenv.2016.03.023, http://www.sciencedirect.com/science/article/pii/S1352231016301935, 2016.

Xie, X., Semanjski, I., Gautama, S., Tsiligianni, E., Deligiannis, N., Rajan, R. T., Pasveer, F., and Philips, W.: A Review of Urban Air Pollution Monitoring and Exposure Assessment Methods, ISPRS International Journal of Geo-Information, 6, 389, https://doi.org/10.3390/ijgi6120389, https://www.mdpi.com/2220-9964/6/12/389, 2017.

Xu, H., Bechle, M. J., Wang, M., Szpiro, A. A., Vedal, S., Bai, Y., and Marshall, J. D.: National PM2.5 and NO2 exposure models for China based on land use regression, satellite measurements, and universal kriging, Science of The Total Environment, 655, 423–433, https://doi.org/10.1016/j.scitotenv.2018.11.125, http://www.sciencedirect.com/science/article/pii/S0048969718344802, 2019a.

Xu, H., Léon, J.-F., Liousse, C., Guinot, B., Yoboué, V., Akpo, A. B., Adon, J., Ho, K. F., Ho, S. S. H., Li, L., Gardrat, E., Shen, Z., and Cao, J.: Personal exposure to $PM_{2.5}$ emitted from typical anthropogenic sources in southern West Africa: chemical characteristics and associated health risks, Atmospheric Chemistry and Physics, 19, 6637–6657, https://doi.org/https://doi.org/10.5194/acp-19-6637-2019, https://www.atmos-chem-phys.net/19/6637/2019/, 2019b.

Yu, X., Stuart, A. L., Liu, Y., Ivey, C. E., Russell, A. G., Kan, H., Henneman, L. R. F., Sarnat, S. E., Hasan, S., Sadmani, A., Yang, X., and Yu, H.: On the accuracy and potential of Google Maps location history data to characterize individual mobility for air pollution health studies, Environmental Pollution, 252, 924–930, https://doi.org/10.1016/j.envpol.2019.05.081, http://www.sciencedirect.com/science/article/pii/S0269749118359049, 2019.